TECHNICAL REPORT
NATICK/TR-92/030

AD A255 128

STUDIES OF A LASER/NUCLEAR THERMAL-HARDENED BODY ARMOR

N.Y. MISCONI
FLORIDA INSTITUTE OF TECHNOLOGY
MELBOURNE, FLORIDA 32901
G.J. CALDARELLA
J.F. ROACH

August 1992

Final Report
January 1991 - September 1991

APPROVED FOR PUBLIC RELEASE; DISTRIBUTION UNLIMITED

UNITED STATES ARMY NATICK
RESEARCH, DEVELOPMENT AND ENGINEERING CENTER
NATICK, MASSACHUSETTS 01760-5000

SOLDIER SCIENCE DIRECTORATE

DISCLAIMERS

The findings contained in this report are not to be construed as an official Department of the Army position unless so designated by other authorized documents.

Citation of trade names in this report does not constitute an official endorsement or approval of the use of such items.

DESTRUCTION NOTICE

For Classified Documents:

Follow the procedures in DoD 5200.22-M, Industrial Security Manual, Section II-19 or DoD 5200.1-R, Information Security Program Regulation, Chapter IX.

For Unclassified/Limited Distribution Documents:

Destroy by any method that prevents disclosure of contents or reconstruction of the document.

DISCLAIMER NOTICE

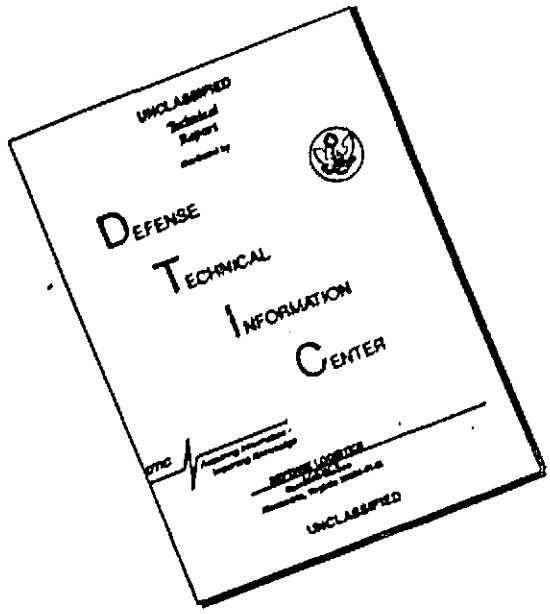

THIS DOCUMENT IS BEST QUALITY AVAILABLE. THE COPY FURNISHED TO DTIC CONTAINED A SIGNIFICANT NUMBER OF PAGES WHICH DO NOT REPRODUCE LEGIBLY.

REPORT DOCUMENTATION PAGE

Form Approved
OMB No 0704-0188

1. AGENCY USE ONLY (Leave blank)	2. REPORT DATE	3. REPORT TYPE AND DATES COVERED
	August 1992	Final 1/31/91 - 9/30/91

4. TITLE AND SUBTITLE
STUDIES OF A LASER/NUCLEAR THERMAL HARDENED BODY ARMOR

5. FUNDING NUMBERS
PE: 62786
PR: 1L1AH98
TA: CABOO
AG CODE: T/B 1257

6. AUTHOR(S)
N. Y. Misconi, Gerald J. Caldarella, Joseph F. Roach

7. PERFORMING ORGANIZATION NAME(S) AND ADDRESS(ES)
Florida Institute of Technology
Department of Mechanical & Aerospace Engineering
Florida Institute of Technology
328 W. Hibiscus Blvd
Melbourne, Florida 32901

8. PERFORMING ORGANIZATION REPORT NUMBER

9. SPONSORING/MONITORING AGENCY NAME(S) AND ADDRESS(ES)
U.S. Army Natick Research, Development and Engineering Center
Kansas Street attn: STRNC-UE
Natick, MA-01760

10. SPONSORING/MONITORING AGENCY REPORT NUMBER
NATICK/TR-92/030

11. SUPPLEMENTARY NOTES

12a. DISTRIBUTION/AVAILABILITY STATEMENT
Approved for public release, distribution unlimited.

12b. DISTRIBUTION CODE

13. ABSTRACT (Maximum 200 words)

The problem of laser/nuclear hardening of body armors and other applications, such as rigid wall, etc, has been investigated in this study. Earlier results from studies of hardening against space systems, which were supported by the Air Force Office of Scientific Research (AFOSR) and carried out by the Principal Investigator during 1984 to 1989 are summarized. The concepts of particle layer and photon multiple scattering inside the layers were utilized in developing a laser shield to protect against laser weapons in the 0.22 to 2.4 micrometer region of the spectrum. Protection against the threats from CO_2 laser weapons are addressed, and the development of a protective shield is detailed. It is now possible to apply a coating that will protect against laser/nuclear threats and reduction of solar loads for 0.22 to 16 micrometers of the spectrum. Applications are expected for rigid walls (Army containers), human body armor, thermal jeckets for military hardware, etc. Finally, a mathematical model was created to help predict how the laser hardening material will behave under specific constraints that have not yet been tested in the laboratory. Also, this model can be used to extrapolate the performance of similar materials/coatings in the mid- to far-infrared wavelengths and also predict the broadband performance.

14. SUBJECT TERMS
LASER BEAMS; LIGHT SCATTERING; PARTICLES; MATHEMATICAL MODELS; BODY ARMOR; SOLID PARTICLES; LASER WEAPONS; MODELS; LASER WEAPONS; NUCLEAR/THERMAL

15. NUMBER OF PAGES
53

16. PRICE CODE

17. SECURITY CLASSIFICATION OF REPORT	18. SECURITY CLASSIFICATION OF THIS PAGE	19. SECURITY CLASSIFICATION OF ABSTRACT	20. LIMITATION OF ABSTRACT
UNCLASSIFIED	UNCLASSIFIED	UNCLASSIFIED	UNCLASSIFIED

TABLE OF CONTENTS

List of Figures

List of Tables

PREFACE

The work described in this report on studies of a laser/nuclear thermal hardened body armor was undertaken during the period January 31, 1991 to September 30, 1991. The professional affiliation of N.Y. Misconi is Center for Geo-Space Environmental Research, Department of Mechanical & Aerospace Engineering, Florida Institute of Technology, Melbourne, Florida. The Natick affiliation of Gerald J. Caldarella and Joseph F. Roach is Physics and Engineering Branch, Fiber and Polymer Division, Soldier Science Directorate.

The funding for this research was Program Element 62786, Project Number 1L1AH98, Task Number CAB00.

The citation of tradenames in this report does not constitute an official endorsement or approval of the use of an item.

The authors are grateful to Marcia Lightbody for her assistance in editing and preparing this document.

STUDIES OF A LASER/NUCLEAR THERMAL-HARDENED BODY ARMOR

SUMMARY

This final report contains three parts. Part I gives the history and background concerning the earlier research supported by the Air Force Office of Scientific Research (AFOSR), during the years 1984 to 1989. This research was under AFOSR's Satellite Survivability Program, which aimed at developing a laser shield to harden space systems against space- and ground-based laser weapons. We used the concept of particle light scattering instead of particle light absorption in developing this shield. The light scattering concept utilized the makeup of a layer of highly irregular μm sized particles that are highly pure. The multiple scattering inside the layer by the photons enables the majority of them (~99%) to be reflected back and away from the target. An 18 watt, continuous wave (CW) argon laser was used in this investigation. This laser shield protects targets against laser weapons from the 0.22 to 2.4μm region of the spectrum.

Part II of the report deals with protecting targets against the CO_2 laser (10.6 μm) by utilizing the same concepts mentioned above. The layers were made out of naturally occurring NaCl particles, which have very low absorption coefficient (~10^{-8} cm^{-1}) in the region of the spectrum between 2 to 16 μm . The natural salt particle layers were subjected to a CO_2, 20 watt, CW laser and found to reject more than ~99% of the incoming radiation.

Part III of this report contains the details of a created mathematical model based on radiative transfer equations to calculate the temperature profile of the layers as they are subjected to incoming radiation. A computer code was developed to perform these model calculations, in FORTRAN, which is included in the report. The computer code accepts input parameters, such as particle sizes, refractive index, absorption coefficient, etc. It outputs parameters, such as the amount of radiation that emerges out of the layers, temperature distribution across the layer, melting threshold, etc. The purpose of the model is to predict the best combinations of parameters to optimize the radiation by these layers.

Part I. RESEARCH ON THE INTERACTION OF SOLID PARTICLES WITH LASER BEAMS

INTRODUCTION AND HISTORY

From 1985 to 1989 funds from the research program "The Interaction of Solid Particles with Laser Beams: Application to the Defense of Satellites", under "The Satellite Survivability Program" (SSP) at the Air Force Office of Scientific Research (AFOSR) were used to build a state-of-the-art Laser-Particle Dynamics facility at the University of Florida. The research resulted in a patent that is pending for the material, process, and later products that involve protecting many types of military targets against lethal laser weapons.

Since the onset of research for finding methods to protect satellites against laser weapons, absorption of the laser energy before reaching the target has been the prevailing approach. Our research, however, was to find a way to scatter the laser beam, so that, at most, only a very small percentage could reach the satellite, thus rendering the weapon harmless. This approach has the advantage that the shield is not damaged in the process of protecting the target, and thus is reusable. Although the main thrust of our research would contribute to the understanding of scattering by a cloud of particles, we also studied closed aggregates of particles, in the form of a "layer", many particles thick and flattened on both top and bottom surfaces. Our research on layer scattering, to date, has emphasized the distribution of scattered light as a function of particle size, layer thickness, and material. It is this layer scattering facet of our research that was shown to be the most promising in the protection of targets from laser beams.

A thin layer of small, highly transparent particles will act like a diffuse mirror when exposed to an incident laser beam (see Annual Report 1 - AFOSR Contract F49620-85-C-0117). The low absorptivity of the material prevents damage to the layer, even when exposed to intensities as high as 1.5 MW/cm^2. We have found it straightforward to create layers no more than 1 mm thick that will scatter more than 99% of the laser radiation back in the direction of the incident beam. The thinness of the layers and their porosity make for a very lightweight shield that would be desirable for human body armor.

The following sections describe the nature of light scattering by a single particle and by many particles packed in a layer. In the former, we try to reproduce the Mie scattering using laser-particle levitation technique. In the latter we measure the angular distribution of the scattered light above and below a well-packed layer of highly irregular silica particles. These measurements are then used to calculate the laser beam suppression ratio by the layer. This ratio is the light intensity measured below the layer (backscattering of the laser beam) divided by the light intensity above the layer. Comparisons of this ratio are made between several types of silica particles, different particle size range, and different layer thickness. The purpose of these comparisons is to optimize the suppression of the laser beam.

THEORETICAL APPROACH TO LIGHT SCATTERING

Theorists still have not been able to solve the problem of light scattering by even a single irregularly shaped particle. In fact, exact solutions are only available for single spheres and small spheroids, and even these require time-consuming computations. To accommodate effects such as interference and diffraction, one must sum the complex amplitudes of each ray entering the layer, taking into account the phase shift across adjacent paths, not just sum the intensity of the beam. With the huge number of randomly

oriented irregular particles, even today's best supercomputers are not sufficient to give an exact solution for multiple scattering in a layer.

Figure 1 shows the theoretical Mie Scattering curve of a highly pure silica sphere of 33.0μm and refractive index n = 1.496, superimposed on the experimental results found from our laser-levitation experiment[1]. Laser-levitation is a technique used at FIT to study light scattering from single particles and sometimes doublets or triplets. The agreement between the experimental values and the theoretical curve is truly remarkable.

The problem of making theoretical scattering functions for an ensemble of particles or a layer of particles can not be solved even with today's fastest supercomputers. To demonstrate the difficulty of this problem, consider the scattering of sunlight from interplanetary dust particles (otherwise known as the zodiacal light). Here we have scattering of sunlight from a cloud of irregularly shaped particles, and the only way to extract information on scattering by these particles is by inverting the brightness integral to obtain an empirical scattering function for the cloud. Figure 2 shows the different empirical scattering curves obtained by different observers using the previously mentioned method. It is obvious that many features of the Mie curve (Fig.1) are totally washed out in Figure 2. There is even doubt on the validity of obtaining an emperical scattering function, since by inverting the brightness integral one has to make assumptions on the particles density distribution and size. Considering the above, we are resigned to the fact that the distribution of light scattered from a layer of particles can be found only by measuring it experimentally.

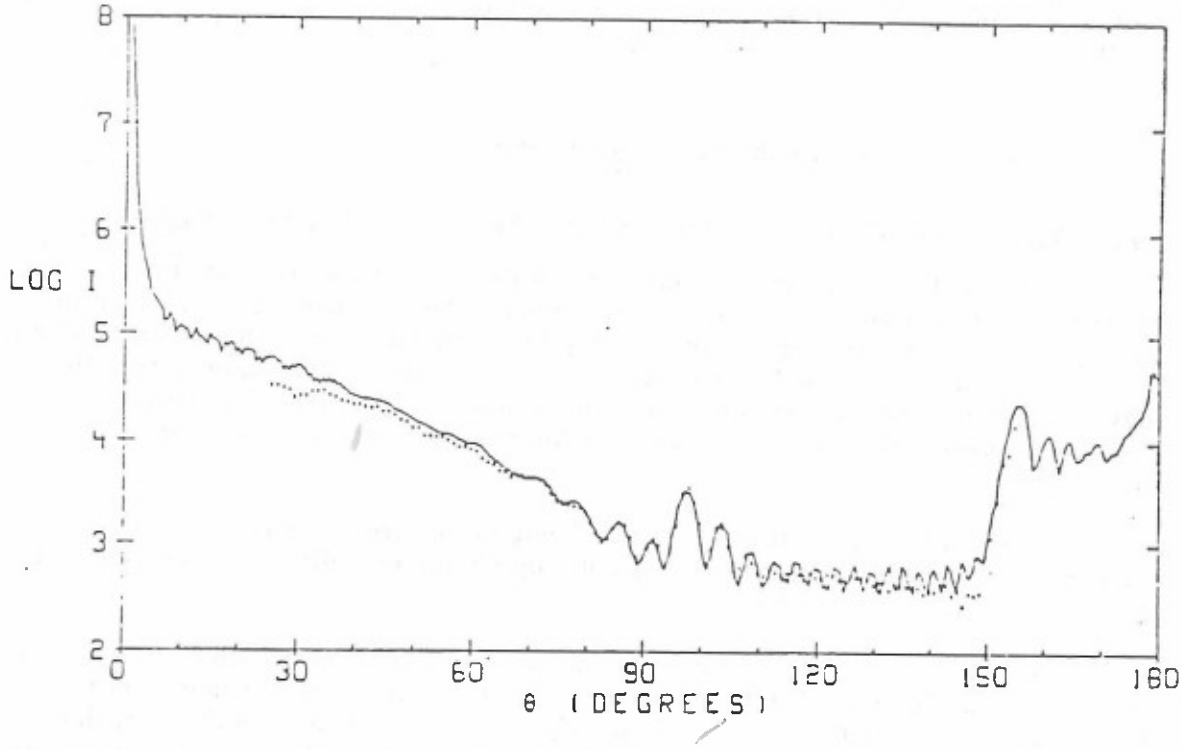

Figure 1. Scattering of 514.5 nm laser light from a 33 μm glass sphere. Measurements (dots) are compared to theory (solid line).

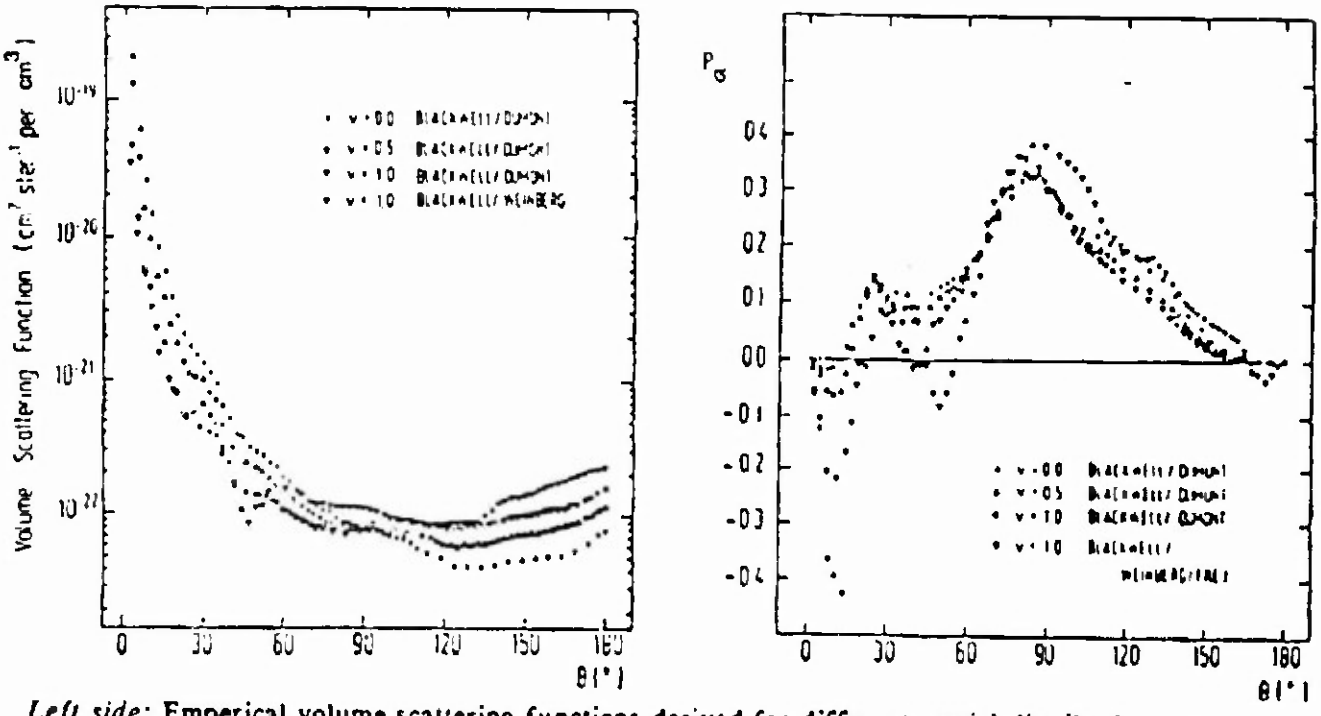

Left side: Emperical volume scattering functions derived for different spatial distribution and different observational data; *Right side:* Degree of polarization of these scattering functions.[3]

Figure 2. Zodiacal light scattering curves.[2,3]

RESULTS: INTERACTION OF SILICATE PARTICLES WITH LASER BEAMS

We tested many different layers of small particles. Each layer was formed from some variety of silicate, be it glass or silicate sand. The sand samples were rinsed in HNO_3 and then distilled water to remove any brine residues. The material was crushed to a fine powder, then sorted into various particle size ranges using sieves from 250 down to 68μm . The particles were then packed into wells built on microscope slides, with depths of 0.25, 0.50, 1, and 2 millimeters, to give layers of these thicknesses.

Particles less than 10μm frequently clung to the larger, sieved particles. We "cleaned" some of these samples by rinsing with distilled water, and left others "dirty" to test the difference.

A silicon photodiode detector was mounted on a goniometer arm and centered in the layer as in Figure 3. The beam of a 20 W argon ion laser was brought from the bottom side of the sample, as shown in the figure, and passed through the glass slide before entering the layer. We retested several samples with the beam incident upon the sample from the top, so that the beam was intercepted by the layer before reaching the slide. There was no difference in the readings.

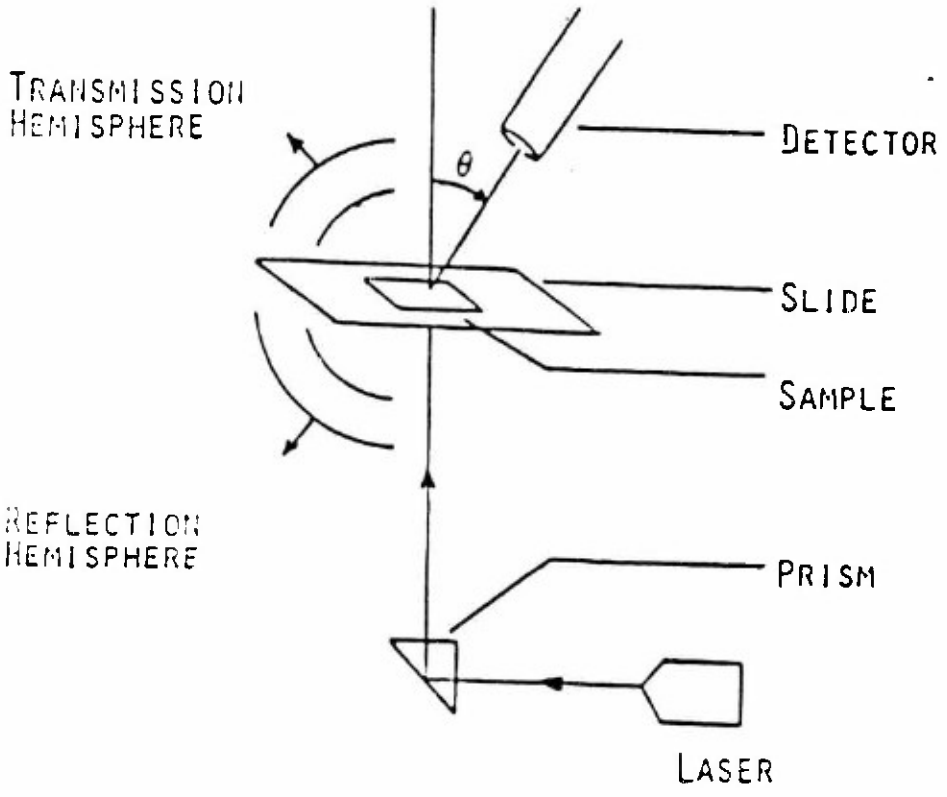

Figure 3. Experimental setup used to measure layer scattering.

Readings were taken by moving the goniometer through scattering angles (Θ) from -165^{0} to $+165^{0}$ (Θ=0 indicated transmission in the direction of the beam). The readings were limited at the high scattering angles by the blocking of the beam by the detector. The scattering, as expected, was symmetric in ±Θ . However, when the layer was tilted we found that the scattering curve became symmetric about a line perpendicular to the layer, and not about the beam axis. An example of a scattering curve is shown in Figure 4a. When corrected for the projection of the surface as seen by the detector, the angular distribution of Figure 4b is obtained. Although the magnitudes of the transmitted and reflected hemispheres varied with particle size and material, the general profile of all of the curves was functionally similar to these in Figure 4.

The scattering curve was extrapolated in the region between 165^{0} and 180^{0} and then integrated to determine the total amount of light reflected vs. the total amount transmitted. This was then reduced to a beam suppression ratio (BSR), where higher numbers refer to a larger amount of light reflected, and thus better protection of a target. Values above 100 were found, but as the BSR increased, the error in measurement also increased, due to the sensitivity limit of our detector. It is conceivable that BSR values greater than 10,000 were achieved, although transmission of such small light levels could not be measured with the apparatus used then.

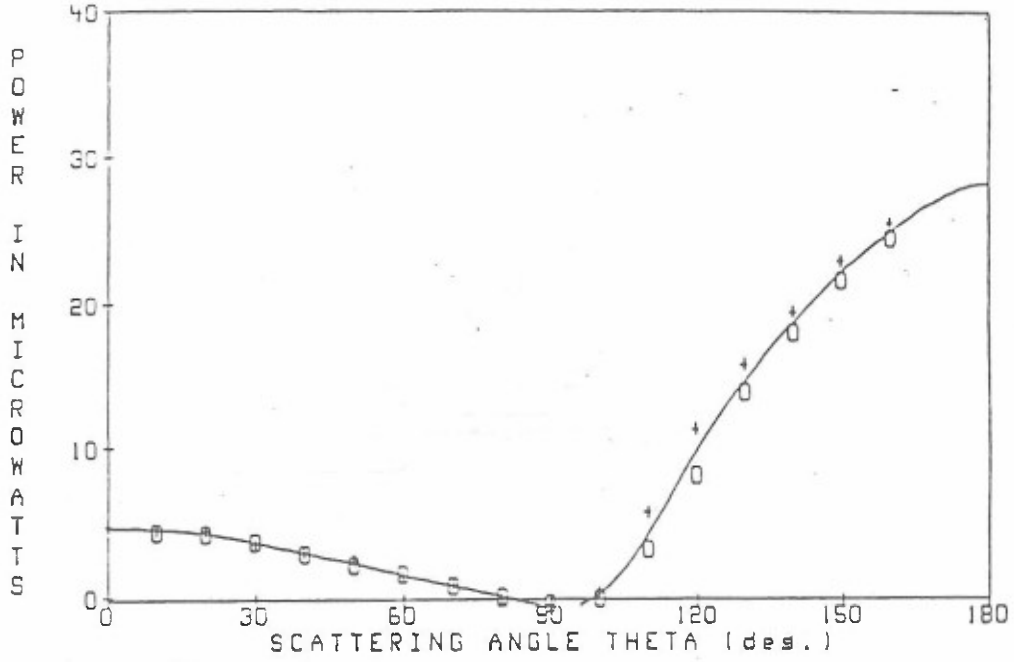

Figure 4a. Scattering and transmission of a 1 mm thick layer of Suprasil™ particles in the size range 90-125μm .

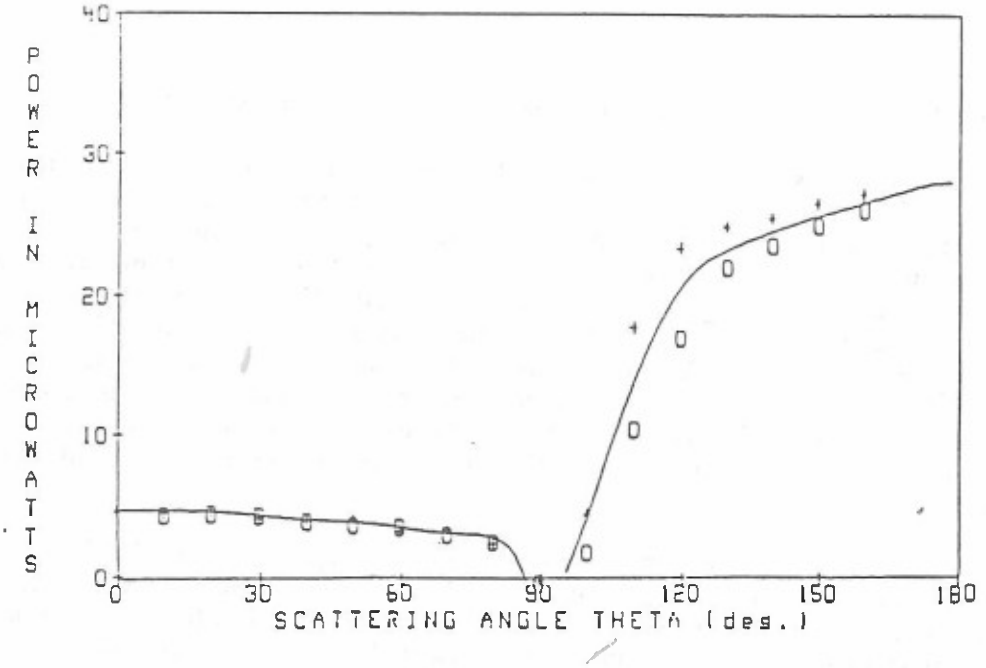

Figure 4b. Scattering and transmission of a 1 mm thick layer of Suprasil particles in the size range 90-125 μm . Here the scattering was adjusted for an effect due to the decrease in the projected spot size at angles close to 90°.

Beam Suppression for Different Types of Glass

Figure 5 shows our experimental results on beam suppression ratios of different kinds of glass and for different layer thicknesses. It leaves no doubt that natural beach sand can give BSR's much better than any man-made glass. It is our contention here that the beach sand gives a higher value of the BSR because it has crystalline structure that is not destroyed in the manufacturing process, not because of an increase in absorption. This structure results in a better light reflection capability for the sand over Suprasil™ and the others. This contention is supported by an X-ray spectroscopy analysis performed at the Department of Materials Science and Engineering of the University of Florida, where measurements of various samples show that some sand samples are more pure than even Suprasil glass.

To test the level of protection afforded by these materials, and indirectly, their absorption, we focused the full power of the laser beam just below the surface of each sample, giving a power density of 1.5 MW/cm^2 of continuous energy for three minutes. Most samples melted under this power, but some survived, including Suprasil glass, which we knew to have a low absorption coefficient. We compared the scattering curves of Suprasil with others that also were undamaged, and found that the naturally occurring sands, which reflected more light than Suprasil to achieve higher BSR's, corresponded to these undamaged samples.

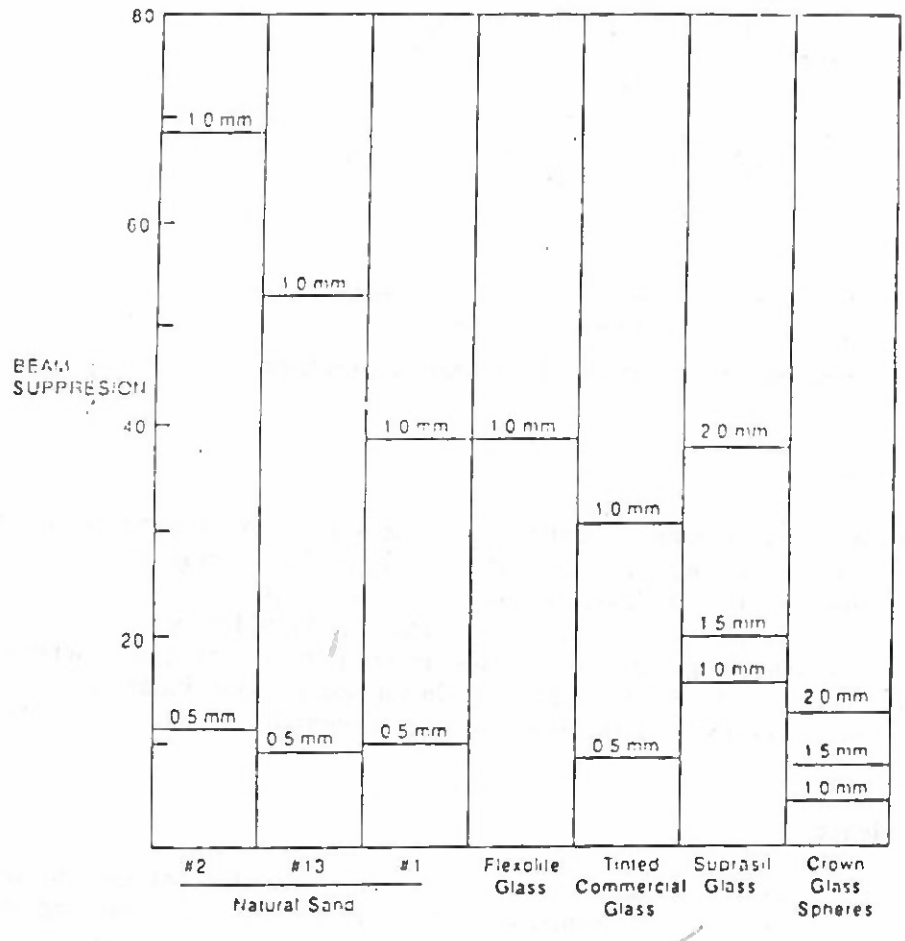

Figure 5. Beam suppression ratios for various materials.

Particle Shape

Our experimental results for the effect of particle shape on the fraction of the laser beam that emerges from the layer in the forward direction are shown in Figure 6. Layers of the same thickness but made up of irregular particles give BSRs a factor of seven higher than equivalently sized spheres. The irregulars reflect the laser beam significantly better than spheres.

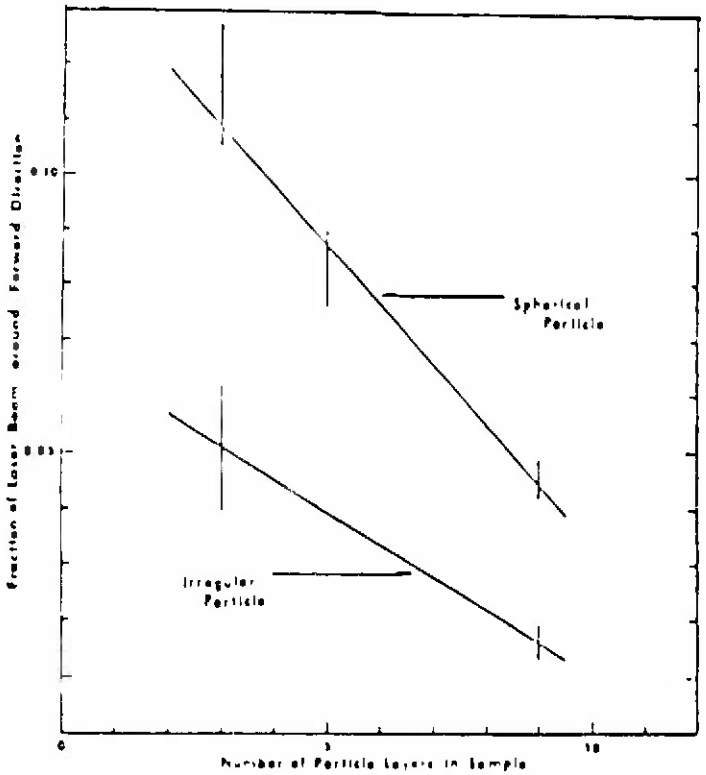

Figure 6. Effect of particle shape and laser beam suppression.

Wavelength Dependence

Our experience with glasses and silicates showed no wavelength dependence (to within the accuracy of our measurements) across the .458 to .514 μm range of our test laser. This, however, is a small fraction of the .22 to 2.2 μm range of transparency for silicates. Theoretically, this material should show a functional dependence on wavelength due to a change in the particle size to wavelength ratio, as well as because of a wavelength dependence in the value of the index of refraction. This conjecture needs to be demonstrated experimentally.

Particle Size Dependence

Our preliminary work demonstrated a strong inverse relationship between the BSR and particle size, which increased more rapidly and nonlinearly toward the small end of our particle size spectrum. The smallest size sieve used in our sizing process was 68μm, This meant that our smallest size range included particles from less than 1μm up to 68μm. While we know that the optimum size range is less than 68μm, more experiments need to be performed to determine if there is a lower limit.

Layer Thickness

More than any other parameter, much is already known about the relationship of layer thickness and beam suppression. In Figure 7 we show the beam suppression ratios of Suprasil as a function of layer thicknesses and also as a function of different sizes. Similarly, in Figure 8 we show the same dependence except for natural sand. Obviously, as thickness increases, less light is transmitted. The one big problem which remains is to relate thickness to absolute numbers for the cases studied above. For example, just how thick does a layer need to be to give a BSR of 10, or of 100, for any given material and size range.

One other question is of interest: does layer thickness affect melting, and if so, how? The total absorption of a layer depends on the thickness of the layer. However, as thickness increases, the total energy absorbed is distributed among more and more particles, and the trade-off between these two effects is not clear. Measurements are needed to determine the effect of layer thickness on melting.

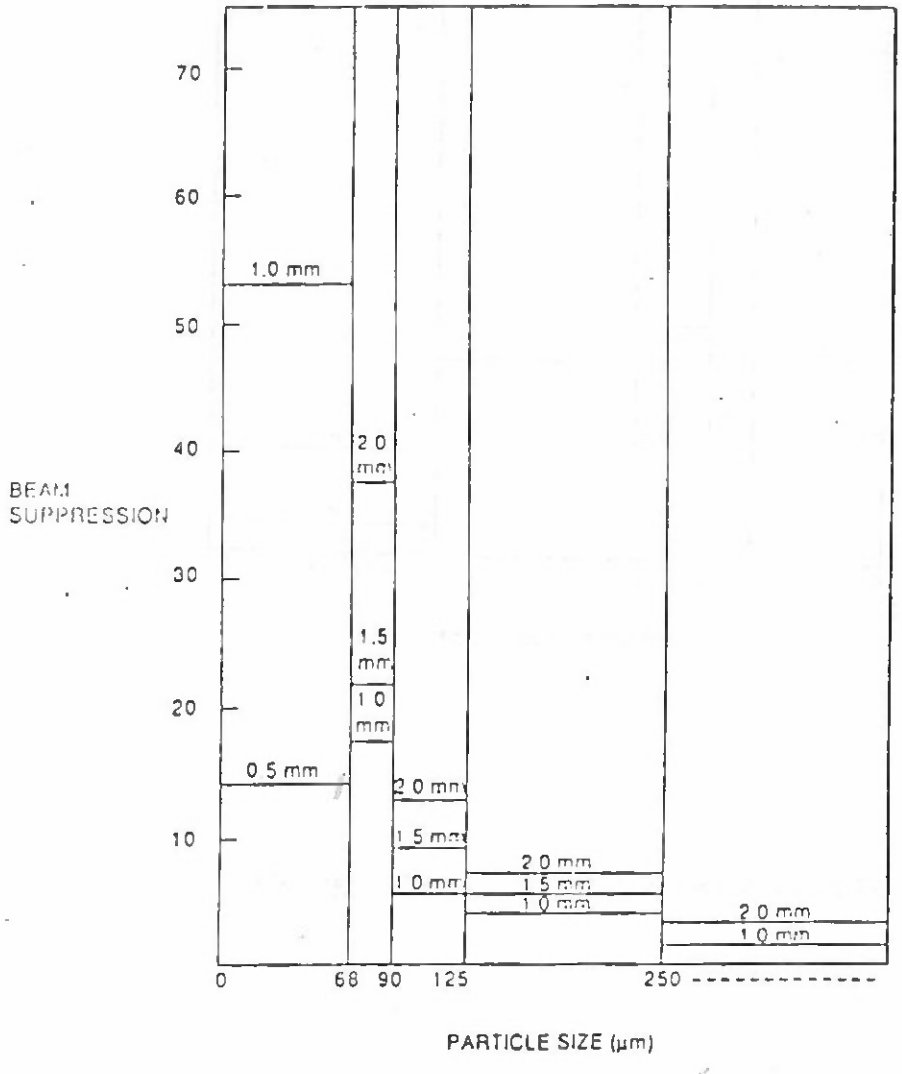

Figure 7. BSR as a function of particle size for layers of Suprasil glass.

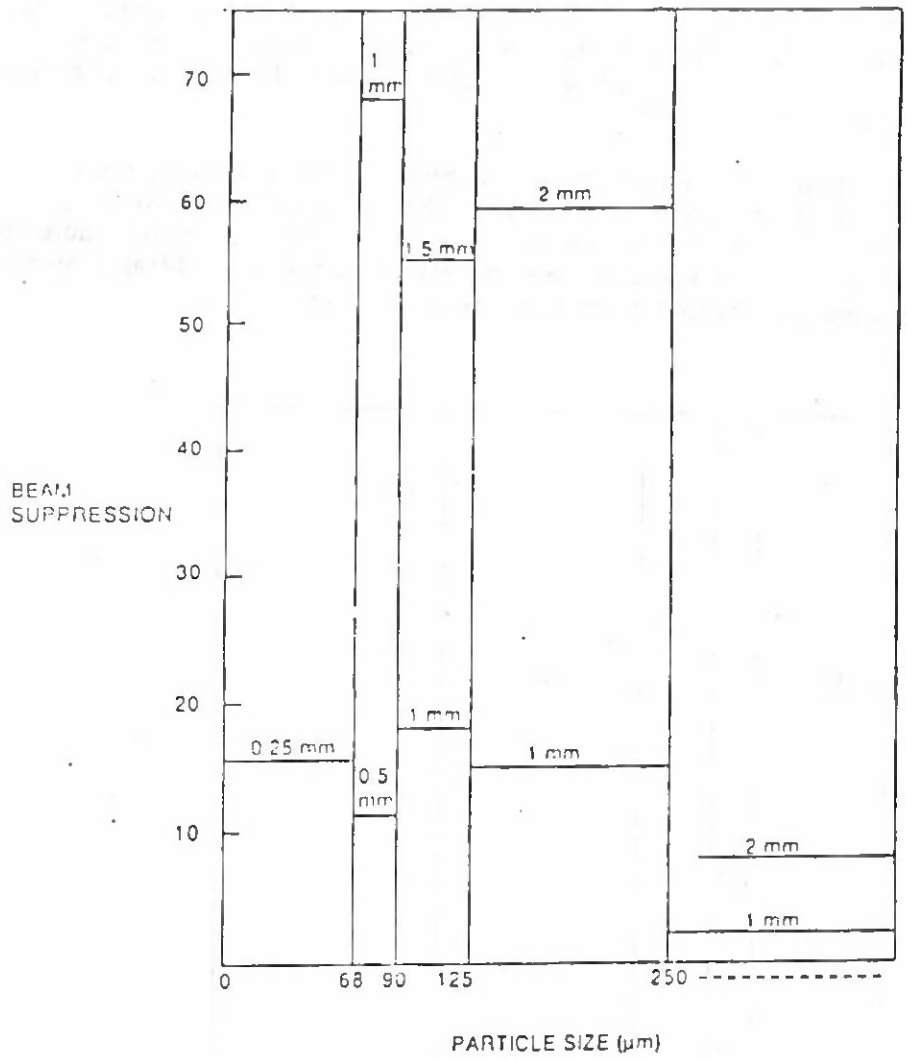

Figure 8. BSR as a function of particle size for natural sand.

Part II. RESEARCH ON LASER/NUCLEAR THERMAL-HARDENED BODY ARMOR

INTRODUCTION

This research project is designed to extend our prior research on scattering by a layer of small (< 250μm) particles to include NaCl particles. A crushed layer of NaCl particles is subjected to the radiation from a 20 watt continuous wave (CW) CO_2 laser to determine the suppression of this radiation for the purpose of using these particles in developing a laser/nuclear thermal hardened body armor. Tests are also made to determine the melting thresholds of these particles under intense radiation. A mathematical model appears in Part III that was developed to optimize the reflectivity by using these particles in various size ranges near the wavelength of the incident laser beam. Prior experiments using highly pure silica particles indicate that we can reject laser light to such a degree that less than one part in 10^4 reaches the target.

The study involves making measurements across a wide dynamic range. Namely, to accurately access the effects of particle size, layer thickness, index of refraction, and wavelength on the distribution of transmitted and reflected light and absorption for very low transmission levels. Our ultimate goal is to create a suitable method utilizing this unique multiple scattering concept to improve the present hardened body armor against nuclear and laser threats.

RESEARCH METHODOLOGY

A detector for very low energy levels, 10^{-9} W, was mounted on a goniometer arm, centered in the layer as in the sketch of Figure 3. The beam of a 20 watt CW CO_2 laser was brought from the bottom side of the sample, as shown in Figure 3, and passed through the zinc selenium (ZnSe) slide before entering the layer.

The CO_2 laser was pulsed to avoid damage to the detector (Pyroelectric* with chopping capability). The parameters used in this computer pulsing are given in Table 1.

TABLE 1

Power Computations of CO_2 Laser. Constant Pulse Repetition Interval is 100 ms

Duty Cycle	Power
%	mW
1	200
2	400
3	600

(Continued)

Table 1 *(Continued)*

4	800
5	1000
6	1200
7	1400
8	1600
9	1800
10	2000
12	2400
14	2800
16	3200
18	3600
20	4000
22	4400
24	4800
26	5200
28	5600
38	7600
48	9600
58	11600
68	13600
78	15600
88	17600
98	19600
100	20000

RESULTS: INTERACTION OF NaCl PARTICLES WITH CO_2 LASER

We used several thicknesses of the layer of particles size 25 μm starting with thickness of 4 mm. We could not detect any radiation coming out of the layer and into the detector i.e., the amount of radiation reaching the detector is in the noise of the detector (< 10^{-8} watts). Similar results were obtained with thicknesses greater than 2 mm. In Table 2, we show the power of the laser beam incident on the layer and the amount of radiation reaching the detector in mW. The beam suppression ratio (BSR) is redefined now as the ratio between output power divided by the input power and is given in Table 2. The BSR ratio is the reverse of the Beam Transmission Ratio (BTR) used before. We chose to do that here by recognizing it is easier to see how much energy is transmitted through the layer and reaching the target. It is clearly obvious that the amount of energy coming out of the layer is negligible in terms of doing any harm to the target, i.e., 10^{-6} to 10^{-5} mW (Tables 2 and 3).

TABLE 2

BTR of NaCl < 250μm Particle Size, 2 mm layer

Time of exposure of the layer to the laser beam = 60 s

Serial #	Power Input	Power Output	Beam Transmission Ratio
	mW	mW	BTR
1	1000	0.008	8.00E-06
2	1200	0.008	6.67E-06
3	1400	0.009	6.43E-06
4	1600	0.010	6.25E-06
5	1800	0.011	6.11E-06
6	2000	0.012	6.00E-06
7	2400	0.013	5.42E-06
8	2800	0.015	5.36E-06
9	3200	0.018	5.63E-06
10	3600	0.019	5.28E-06
11	4000	0.024	6.00E-06
12	5600	0.036	6.43E-06
13	7600	0.047	6.18E-06
14	9600	0.060	6.25E-06
15	20000	0.113	5.65E-06

TABLE 3

BTR of NaCl - Particle Size = 25μm, 1 mm Layer

Time of exposure of the layer to the laser beam = 60 s

Serial #	Power Input	Power Output	Beam Transmission Ratio
	mW	mW	BTR
1	1000	0.027	2.70E-05
2	1200	0.034	2.83E-05
3	2000	0.056	2.80E-05
4	4000	0.114	2.85E-05
5	7600	0.221	2.91E-05
6	9600	0.308	3.21E-05
7	20000	0.836	4.18E-05

In Table 4 we show the results for layer thickness of 0.5 mm. Again we see that the amount of energy transmitted through the layer is insignificant. This fact is really remarkable, since 0.5 mm is equivalent to 500μm thickness of a layer of approximately 25μm particles, which in turn means few particles thick. We are not able at this time to determine values for layer thicknesses < 0.5 mm, for the difficulty in making them. We would like to determine these values in a continuation study that would enable us to devise methods of making thin (< 0.5 mm) layers.

TABLE 4

BTR of NaCl - 25μm Particle Size, 0.5 mm layer.

Time of exposure of the layer to the laser beam = 60 s

Serial #	Power Input	Power Output	Beam Transmission Ratio
	mW	mW	BTR
1	1000	0.130	1.30E-04
2	1200	0.164	1.37E-04
3	1400	0.185	1.32E-04
4	2000	0.230	1.15E-04
5	4000	0.284	7.10E-05
6	5600	0.280	5.00E-05
7	7600	0.311	4.09E-05
8	9600	0.361	3.76E-05
9	15600	0.996	6.38E-05
10	17600	1.830	1.04E-04
11	19600	3.360	1.71E-04
12	20000	3.100	1.55E-04

We include here measurements made using layers of particles with sizes higher than 25 μm in order to see if larger sizes of the particles will affect the reflectivity of the layer and if so by how much:

TABLE 5

BTR of NaCl - 40μm Particle Size, 0.5 mm Layer

Time of exposure of the layer to the laser beam = 60 s

Serial #	Power Input	Power Output	Beam Transmission Ratio
	mW	mW	BTR
1	1000	0.16	1.60E-04
2	1200	0.18	1.50E-04
3	2000	0.24	1.20E-04
4	4000	0.44	1.10E-04
5	5600	0.6	1.07E-04
6	7600	0.8	1.05E-04
7	9600	0.98	1.02E-04
8	15600	1.5	9.62E-05
9	17600	1.72	9.77E-05
10	19600	1.73	8.83E-05
11	20000	1.78	8.90E-05

TABLE 6

BTR of NaCl - 40μm Particle Size, 0.5 mm Layer

Time of exposure of the layer to the laser beam = 60 s

Serial #	Power Input	Power Output	Beam Transmission Ratio
	mW	mW	BTR
1	1000	0.32	3.20E-04
2	1200	0.36	3.00E-04
3	1400	0.4	2.86E-04
4	2000	0.49	2.45E-04
5	4000	0.95	2.38E-04
6	5600	1.32	2.36E-04
7	7600	1.74	2.29E-04
8	9600	1.93	2.01E-04
9	15600	2.91	1.87E-04
10	17600	3.31	1.88E-04
11	19600	3.37	1.72E-04
12	20000	3.46	1.73E-04

TABLE 7

BTR of NaCl - 53μm Particle Size, 0.5 mm Layer

Time of exposure of the layer to the laser beam = 60 s

Serial #	Power Input	Power Output	Beam Transmission Ratio
	mW	mW	BTR
1	1000	0.34	3.40E-04
2	1200	0.42	3.50E-04
3	2000	0.56	2.80E-04
4	4000	1.07	2.68E-04
5	5600	1.33	2.38E-04
6	7600	1.84	2.42E-04
7	9600	2.18	2.27E-04
8	15600	3.29	2.11E-04
9	17600	3.64	2.07E-04
10	19600	3.65	1.86E-04
11	20000	3.68	1.84E-04

TABLE 8

BTR of NaCl - 90μm Particle Size, 0.5 mm Layer

Time of exposure of the layer to the laser beam = 60 s

Serial #	Power Input	Power Output	Beam Transmission Ratio
	mw	mw	BTR
1	1000	0.32	3.20E-04
2	1200	0.36	3.00E-04
3	2000	0.62	3.10E-04
4	4000	1.15	2.88E-04
5	5600	1.62	2.89E-04
6	9600	2.49	2.59E-04
7	15600	3.64	2.33E-04
8	17600	4.28	2.43E-04
9	19600	4.34	2.21E-04
10	20000	4.48	2.24E-04

TABLE 9

BTR of NaCl - 125μm Particle Size, 0.5 mm Layer

Time of exposure of the layer to the laser beam = 60 s

Serial #	Power Input	Power Output	Beam Transmission Ratio
	mw	mw	BTR
1	1000	0.47	4.70E-04
2	1200	0.5	4.17E-04
3	2000	0.72	3.60E-04
4	4000	1.26	3.15E-04
5	5600	1.68	3.00E-04
6	9600	2.85	2.97E-04
7	15600	4.45	2.85E-04
8	17600	4.73	2.69E-04
9	19600	4.92	2.51E-04
10	20000	5.13	2.57E-04

TABLE 10

BTR of NaCl - 250μm Particle Size, 0.5 mm Layer

Time of exposure of the layer to the laser beam = 60 s

Serial #	Power Input	Power Output	Beam Transmission Ratio
	mw	mw	BTR
1	1000	0.23	2.30E-04
2	1200	0.33	2.75E-04
3	2000	0.45	2.25E-04
4	4000	0.91	2.28E-04
5	5600	1.22	2.18E-04
6	9600	1.96	2.04E-04
7	15600	3.06	1.96E-04
8	17600	3.19	1.81E-04
9	19600	3.46	1.77E-04
10	20000	3.48	1.74E-04

Part III. LASER/NUCLEAR HARDENING SCATTER EFFICIENCY MODEL

This Part presents a mathematical model for the properties of a silica-based particle layer used as a laser shield. Heat flow and beam attenuation models are derived, then combined in a computer program. The computer model predicts maximum survivable power density levels for varying materials and shield configurations. In addition, the heat flow model provides temperature profiles across the shield layer resulting from laser energy absorption, and the beam attenuation model provides beam absorption, reflection and transmission as a function of layer material and thickness.

These models are intended to provide an initial theoretical framework to predict/extrapolate performance beyond the current experimental boundaries. Specifically, the model can be used to extrapolate the performance of similar materials/coatings in the mid-to-far infrared wavelengths, and to predict broadband performance. Significant work remains to experimentally verify and expand the results obtained to date, and to further develop the model framework begun here.

The authors of this model continue to stress the wide variety of applications of this laser hardening to satellites. satellite solar panels. missile boosters and nose cones. SDI deployed systems, and others.

MODEL INPUTS

1. particle size (s).

2. particle shape: highly irregular.

3. particle refractive index (n).

4. particle absorptivity as a function of wavelength a(l).

5. powder packing fraction (PF = % of solid material).

6. particle material thermal-physical propertics:
   density (r), melting temperature T_m , thermal diffusivity (a) which is equal to thermal conductivity (k) divided by the heat capacity (c), and density (r).

7. layer thickness (x).

8. type of laser beam (CW vs. pulsed): assumed CW for duration of time on target.

9. wavelength (l).

10. laser power density (P)

MODEL OUTPUTS

1. amount of forward scattering or transmission of laser light through the layer.
2. amount of retroscattering or reflection of laser light from the layer.
3. temperature distribution across the layer.
4. melting/damage threshold of the laser shield.
5. bulk absorption through the layer.

TEMPERATURE PROFILE MODEL

Here we examine the flow of heat in the coating and, in particular, the resulting temperature profile. For our purpose, which is to obtain a worst-case prediction, a relatively simple mathematical model is sufficient to describe the basic features of the interaction of a laser beam with the coating. To begin with, we assume that the coating is an infinitesimally thin homogeneous and isotropic medium with thermal conductivity k, density ρ, and specific heat c. As the coating is essentially two-dimensional, the temperature distribution throughout the coating is governed by the two-dimensional heat equation

$$\frac{1}{r}\frac{\partial}{\partial r}\left(r\frac{\partial T}{\partial r}\right)+\frac{1}{r^2}\frac{\partial^2 T}{\partial \theta^2}+\frac{1}{k}g(r,\theta,t)=\frac{1}{\alpha}\frac{\partial T}{\partial t} \qquad (1)$$

In the above, $T(r,\theta,t)$ is the temperature at the point (r,θ) (in polar coordinates) at the time t. The parameter α is given by $\alpha = k/\rho c$. The function $g(r,\theta,t)$ is the rate of heat generation per unit volume.

The heat equation is a parabolic differential equation and needs to be supplemented with boundary conditions and an initial condition. We assume that the boundary is a circle at r=R at which no heat can enter or escape:

$$\left.\frac{\partial T}{\partial r}\right|_{r=R}=0\,. \qquad (2)$$

At t=0, we assume that the layer is at a constant temperature T_0. Without loss of generality, we can define T to be measured relative to this initial temperature (this is permissible since both the heat equation (1) and our boundary condition (2) are linear), then the initial condition is

$$T(r, \theta, 0) = 0 . \tag{3}$$

If we choose our coordinates such that the beam is centered at the origin, then azimuthal symmetry implies that T is independent of θ and equation (1) reduces to

$$\frac{1}{r}\frac{\partial}{\partial r}\left(r\frac{\partial T}{\partial r}\right) + \frac{1}{k}g(r, t) = \frac{1}{\alpha}\frac{\partial T}{\partial t} \tag{4}$$

This equation is solved by expanding the radial dependence of T (r,t) in terms of Bessel functions, the precise form of the expansion is controlled by the boundary condition (2). Equation (4) reduces to a linear, first-order ordinary differential equation in the time which is easily solved in conjunction with the initial condition (3). The solution takes the form

$$T(r, t) = \sum_{m=0}^{\infty} e^{-\omega\beta_m^2 t} K_0(\beta_m r)\int_0^t du\, A(\beta_m, u) , \tag{5}$$

where

$$K_0(\beta_m, r) = \frac{\sqrt{2}}{R}\frac{J_0(\beta_m r)}{J_0(\beta_m R)} , \tag{6}$$

and

$$A(\beta_m, u) = \frac{\alpha}{k}\int_0^R dr\, r\, K_0(\beta_m, r)\, g(r, t) . \tag{7}$$

The functions J_0 are zeroth-order Bessel functions. The constants β_m are the roots of the equation

$$\left.\frac{dJ_0(\beta r)}{dr}\right|_{r=R} = 0$$

To proceed further, we need to choose a form for g(r,t). Again, for our purposes, the simplest choice suffices. We model the laser beam as a point source of constant integrated power γ located at r=0. Mathematically, this is accomplished by choosing g(r,t) as

$$g(r, t) = \frac{\gamma}{2\pi r}\delta(r), \tag{8}$$

where δ(r) is Dirac's delta distribution. The integral over r in (7) can then be performed:

$$A(\beta_m, t) = \frac{\alpha\gamma}{\sqrt{2}\,\pi R}\frac{1}{J_0(\beta_m R)} . \tag{9}$$

This then allows us to perform the integral in u in (5) to get

$$T(r,t) = \left(\frac{\alpha\gamma}{\pi k R^2}\right) t + \sum_{m=1}^{\infty} \left(\frac{\gamma}{\pi k}\right) (\beta_m R)^{-2} \frac{J_0(\beta_m r)}{J_0^2(\beta_m R)} \left(1 - e^{-\alpha\beta_m^2 t}\right). \tag{10}$$

The first term in (10) is the dominant effect of the boundary and represents a linear build up of heat in time. The remaining infinite series is the exponential approach to late-time equilibrium (obtained by setting the exponential term to zero).

We evaluate (10) numerically below, but a useful approximation can be devised. Assume the medium is large ($\beta R >> 1$), and that we observe the temperature near the beam, i.e., $\beta r << 1$, then using the asymptotic forms for the Bessel functions yields

$$T(r,t) \cong \left(\frac{\alpha\gamma}{\pi k}\right) t + \frac{\gamma}{2k}\left[\sum_{m=1}^{n} \frac{1}{\beta_m^2}\left(1 - e^{-\alpha\beta_m^2 t}\right) + \sum_{m=n}^{\infty} \sqrt{\frac{2}{\beta_m^3 r}}\left(1 - e^{-\alpha\beta_m^2 t}\right)\cos\left(\beta_m r - \frac{\pi}{4}\right)\right]. \tag{11}$$

The cosine term in (11) will slowly vary between ± 1. The sum will converge due to the $\beta^{-3/2}$ term which can be approximated by $(m\pi)^{-3/2}$. (In (11) we renormalized our distance scale such that R=1.) For small r, $m_1 = R/4r$, e.g. For R=1 cm and r=.01 cm, $m_1 = 25$. For quartz, $\alpha = .002$ cm^2/s, so for $t > 1$ s, $\beta_m^2 > 1000$ will give an exponent < -2, implying that the exponential term can be neglected for m>10.

For higher temperatures, radiative cooling will provide a small but significant contribution to the thermal distribution. Inclusion of this term does not readily yield an analytical solution, but for numerical purposes this can be estimated by taking the time derivative of T(r,t), and subtracting a term dependent on the local temperature. In general this term will be proportional to the integral of the emission function $\epsilon(\lambda)$ over all wavelengths. For a blackbody, $\epsilon(\lambda) = b(\lambda)$, the Planck function, and the integral is:

$$\int b(\lambda)\, d\lambda = \sigma T^4,$$

where σ is the Stefan-Boltzmann constant. Thus for a blackbody,

$$\frac{dT}{dt} = \frac{\alpha\gamma}{\pi k} + \frac{\alpha\gamma}{2k} \sum_{m=1}^{\infty} e^{-\alpha\beta_m^2 t} - \frac{\sigma}{\rho c} T^4 \tag{12}$$

Although transparent materials are poor approximations to a blackbody, the radiative term is small. The computer model, discussed below, ignores the radiative cooling term in its

present implementation, which yields a more conservative estimate of shield resistance to melting.

BEAM ATTENUATION MODEL

This section deals with the theory of the relation between reflection, transmission, and absorption to layer thickness. We will define the parameters upon which the theory depends, and use these to determine a thickness which will give a reasonable level of protection to the substrate.

In general, we wish to minimize the thickness (x) (and thus the weight) of the shield, while maximizing the fraction of light reflected (R) and minimizing the fractions of both the absorbed (A) and transmitted (T) light. Using basic principles, we can derive the equations relating these quantities. We assume that for some thickness x, the values are known. Then, by increasing the thickness of the layer by an additional δx, we solve for the changes in these quantities. By making δx small enough, we can assume linearity in reflection and absorption so that

$$T(\delta x) = 1 - c_T \delta x$$
$$R(\delta x) = c_R \delta x$$
$$A(\delta x) = c_A \delta x$$
$$A + R + T = 1, \tag{13}$$

where c_R, c_T, and c_A are coefficients of reflection, transmission, and absorption, respectively, and have units of inverse length. These are related such that $c_T = c_R + c_A$. Then, using multiple scattering, we get

$$T(x + \delta x) = T(x)(1 - c_T \delta x) + T(x)R(x)c_R \delta x(1 - c_T \delta x) + \cdots$$
$$R(x + \delta x) = R(x) + T^2(x)c_R \delta x + T^2(x)R(x)c_R(\delta x)^2 + \cdots$$

or

$$\frac{dT}{dx} = c_1 RT - c_1 T, \tag{14}$$

$$\frac{dR}{dx} = c_1 T^2, \tag{15}$$

Equations (13) (15) can be solved to give:

$$T = \frac{(q^2 - 1)e^{c_1 x}}{q^2 e^{2c_1 x} - 1} \tag{16}$$

$$R = \frac{q(e^{2cx} - 1)}{q^2 e^{2cx} - 1} \tag{17}$$

$$A = \frac{(q - 1)(e^{cx} - 1)}{qe^{cx} + 1} \tag{18}$$

where $c = (c_T^2 - c_R^2)^{1/2}$, and $q = (c_A + c_R + c) / c_i$. Define x_0 as the thickness where half the light is transmitted; then $x_0 = 1$ when $c_i = 1$. If there were no absorption, then

$$\frac{R}{T} = \frac{x}{x_0} . \tag{19}$$

In the limit of an infinitely thick layer,

$$A = (2A_0)^{1/2} \tag{20}$$

where the subscript "o" denotes the absorption of a layer of thickness x_0. A_0 is approximately equal to $c_A x_0$ when c_A is small.

Because absorption increases with increasing thickness (to a limit) and transmission decreases, some reasonable criterion must be set. To minimize the sum of absorption plus transmission seems reasonable at first, but this sum will always decrease, albeit insignificantly, as the thickness increases. Let us define the "ideal" thickness (x_i), as that where A = T. Beyond this thickness, the absorbed energy dominates the damage potential. This is not to say that increasing the thickness will increase the damage potential, since the absorbed energy per unit mass will decrease. Nonetheless, setting T = A will give us a suitable criterion to work with. Substituting the expressions in equations (4) and (6) and solving for x gives:

$$x_i = \frac{1}{c}\left\{\ln\left[(q + 1) + \sqrt{(q + 1)^2 - 1}\right] - \ln q\right\} \tag{21}$$

Given c_A / c_T, this can be solved for x. A simple approximation is also available. Absorption is nearly linear with thickness for $x < x_0$ and transmission approximately inversely proportional to thickness. So we can get a quick estimate of the thickness for maximum beam suppression:

$$x_i = x_0 A_0^{-1/2} . \tag{22}$$

For example, if $A_0 = 10^{-4}$, then the estimated ideal thickness is $100\ x_0$, at which point both absorption and transmission are 1% of the total radiation. The numbers for the exact solution come out slightly better, absorption = transmission = 0.81% for a thickness of $92.6\ x_0$.

We can minimize the thickness of the layer by minimizing x_0. This can be done to a limited extent by scaling down the sizes of the particles. Eventually, in the limit, the

particles become smaller than the wavelength of the radiation, and their scattering properties change. Still, if x_0 is 10 particle thicknesses, then use of 1 μm particles gives a total layer thickness of less than 1 mm in the above example.

There is a theoretical reason to believe that when particle size is decreased, the corresponding decrease in x_0 is better than linear. This is due to the fact that the smaller the particle, the less peaked are the scattering curves in the forward direction. It would take a several-particles-thick layer of large particles to generate the equivalent backscatter of a monolayer of small particles.

MODEL IMPLEMENTATION

The model equations derived above have been incorporated into a computer program. Fortran source code for this program is presented in Appendix C. Most input parameters are requested at program initiation. However, the thermal-physical constants of the material must be changed in the code itself, if a material other than silica is used. See Appendix A for the parameter input sequence and default values. The program iterates to compute the power density required to bring the layer to 99.5% of the specified melting temperature, within the specified time the beam is on target. This power density is then presented as the resulting "maximum power density" the shield can withstand given the specified input conditions. See Appendix B for a sample output of the model.

The effect of certain properties of the material on the transmission and heating of the layer are presently unknown. Many of these relationships are planned subjects of our proposed experimental study. To facilitate the creation of a model, we have estimated the functional dependences described below.

The effect of particle size was decoupled into two separate forms. The geometric assumption was that an n-particle thick layer scatters with equal efficiency, independently of the size of the particle. Superimposed on this was the assumption that the closer the size of the particle is to the wavelength of the incident beam, the more efficiently it scatters away from the forward direction cf. van de Hulst, 1957[5]. The difference includes both an increase in the ratio of true scattering cross section to geometric scattering cross section (a factor of two at $s=\lambda$; Spitzer, 1968[4]) and an effect due to the increase in isotropy of the scattering curve of small particles over large particles. This was approximated by

$$c_T \propto \frac{1}{s}\left(\frac{\lambda}{s} + \log\frac{s}{\lambda}\right)^{-1} \qquad (24)$$

where c_T is inversely proportional to the thickness needed for 50% reflection, so that a larger value of c_T means a more efficient scatterer.

The index of refraction was also expected to play a role in the scattering efficiency, based on Mie scattering data. This was modeled by

$$c_T \propto \frac{n-1}{n} \qquad (25)$$

to give a number varying between zero (n=1) and one (n infinite).

Finally, it was assumed that the maximum density of interfaces is provided by a layer of 75% solid material, with a higher density allowing faces to overlap and a lower density allowing excess air (or vacuum) space. c_T must go to zero when the layer is all air (PF=0) or solid material (PF=1). Using a cubic to model this property and combining these expressions gives:

$$c_T = \frac{9\,PF\,(n-1)(-8\,PF^2 + 11PF - 3)}{n\,(\lambda + s\log\frac{s}{\lambda})}, \qquad (25)$$

where the 9 is a normalizing term, based on a conservative fit to our previous experimental results.

The program will allow either the thickness or the maximum percentage transmission to be input. If both are set to zero, the code will calculate the default thickness where Transmission = Absorption.

Radiative cooling has been eliminated in the current implementation by setting the Stefan-Boltzmann constant to zero. This gives a lower limit on the resulting maximum survivable power density.

SAMPLE PROGRAM RESULTS

We like to acknowledge here the efforts of Dr. Edwin T. Rusk and Dr. Charles G. Torre at FIT in developing the mathematical treatment and the computer coding of this model. Appendix B provides a sample output of computer model results. The example temperature distribution is for 2 seconds in steps of .01 s. It was generated for a beam of .01 cm diameter centered on a layer 1 cm in radius and set the maximum temperature at the melting point of quartz. Otherwise, the default parameters of the model were used. These include an absorption coefficient of 5×10^{-4}/cm, particles 1 μm in diameter, a wavelength of 488 nm, an index of refraction of 1.46, and a packing fraction of 75%. See Figure 9 for a graphic presentation of the results.

The program iterates on beam power density to produce a temperature of 1873.6K (99.5% of 1883K, the melting point) after 2 seconds. Thus, the computed maximum power density of 34.6 MW/cm^2 is the power density the shield can withstand for two seconds without melting. **Note that the ideal layer thickness computation to provide Transmission = Absorption resulted in a layer of 0.932mm and a transmission/absorption of 0.04%.**

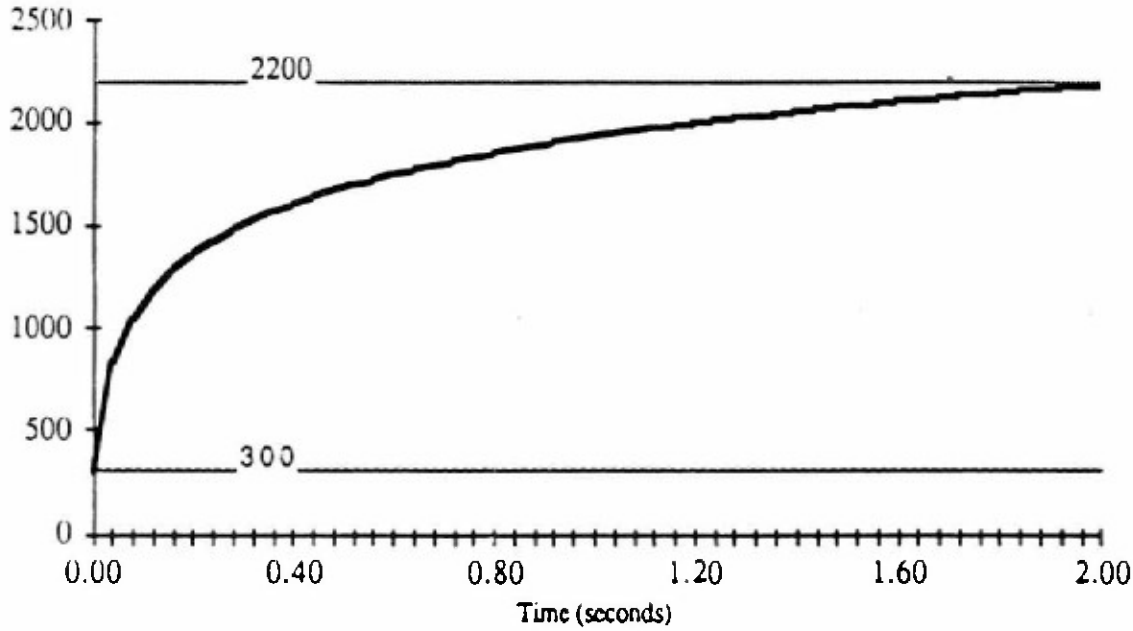

Figure 9: Plot of temperature (Kelvin) at beam edge (.005 cm radius) over the 2 second beam exposure, as presented in Attachment B.

CONCLUSION

These experiments proved that it is possible to reject more than 99.9% of the argon laser beam using highly pure natural occurring beach sand in Florida. This rejection was accomplished by packing highly irregular particles in thin layers (0.5, 1.0, 1.5, and 2.0 mm), which then creates a multiple scattering medium for the laser beam. The absorption coefficient of these highly pure silica particles is of the order of 4×10^{-5} cm^{-1}, which makes them resistant to melting by the laser energy. This rejection of the radiation away from the target is feasible between 0.22 to 2.4 μm wavelength. In this research task, we embarked on extending this method to reject more than 99.99% of the radiation from the beam of a 20 Watt CO_2 CW laser, using NaCl (natural occurring salt). This extends our methodology to reject radiation away from the target from 0.22 to 15μm region of the spectrum.

The CW, CO_2 laser's beam transmission ratio, BTR (the ratio of the energy transmitted to the target divided by that reflected away from the target, see Figure 1), is the reverse of BSR that we used in the initial experiments with silica particles. We preferred to use BTR since it shows readily how small is the energy reaching the target. Tables 2 to 10 show clearly the insignificant amount of energy reaching the target. We were pleasantly surprised as to how well NaCl particles reflected the energy from the CO_2 laser using very thin layers < 0.5 mm, compared to the silica particles layers. We suspect that the reason for that is the long wavelength (10.6 μm) of the photons coming out of the CO_2 laser, and their increased inability to emerge out of the layer compared to the photons in the visible.

Natural NaCl has an absorption coefficient of approximately 10^{-7} cm^{-1}. This very low absorption, from 2 to 15μm wavelength, ensures that this laser shield will not melt or sublimate easily. We have subjected layers of thicknesses 0.5, 1.0, 1.5, 2.0, and 4.0 mm to energy density of approximately 1.5 KW/cm^2 (the limit of our focused CW CO_2 laser beam) and did not notice any melting. FIT likes to test for melting at higher energy densities and will be awaiting the use of the 2.5 KW, CO_2 laser at Natick RD & E Center for such tests.

We also experimented with adhering the highly irregular NaCl particles in the layer, using commercial adhesives. The best adhesive we have used so far is the commercially available polyurethane spray adhesive. The application of our laser/nuclear shielding is fairly easy for rigid wall hardening. The application of our shield on body armor is more complicated due to the fact that it must be applied in a way that keeps the body armor flexible and comfortable. Using this coating material on body armor is subject to more research if the needs of the Army demand hardening against CO_2 laser threats and nuclear threats as well.

Currently, we are exploring the use of our coating to reduce the solar load off Army containers and canisters (rigid walls). The same method with which we reject the radiation from laser beams can be applied to reflecting most of the solar spectrum thus making the environment cooler in hot battlefields such as those encountered in the Desert Shield and Desert Storm operations in Saudi Arabia and southern Iraq. NaCl will reflect the infrared part of the solar spectrum and natural highly pure silica (Florida beach sand) rejects the solar spectrum from 0.22 to 2.4μm. We have not tested this coating against the solar spectrum below 0.22μm; however, application of this coating on rigid walls and exposing it to sunlight should demonstrate its effectiveness in this region of the solar spectrum.

Polyurethane as adhesive proved to be flexible on metal surfaces. It resists cracking due to twisting or bending of the metal. The coating is light weight, approximately 1.2 kg/m^2 when 0.5 mm in thickness.

We hope that our findings from this research task will prove to be very useful for the U.S. Army's defensive applications in the battlefield theater against laser and nuclear threats.

REFERENCES

1. N.Y. Misconi, J.P. Oliver, K.F. Ratcliff, E.T. Rusk, and Wan Xian Wang (1990), "Light Scattering by Laser Levitated Particles". Applied Optics, 29, No. 15, 2276-2281.

2. C. Leinert, H. Link, E. Pitz, R.H. Giese (1976) "Interpretation of a rocket photometry of the inner zodiacal light". Astron. Astrophys. 47, No. 2, Pt. 1, 221-230.

3. J.A.M. McDonnell (1978) Cosmic Dust, John Wiley and Sons.

4. L. Spitzer, Jr. (1968) Diffuse Matter in Space, Interscience Publishers, John Wiley & Sons, New York.

5. H. C. van de Hulst (1957) Light Scattering by Small Particles, John Wiley & Sons, New York.

Appendix A: Parameter Input Sequence

```
ENTER THE MAXIMUM ALLOWABLE TEMPERATURE, ELSE 2200.00K
1883.
THE DIAMETER OF THE BEAM, ELSE   0.100 cm
.01
THE DIAMETER OF THE LAYER, ELSE    1.00 cm
2.
THE TIME THE BEAM IS ON TARGET, ELSE   10.00 sec
2.
THE TIME INCREMENT, ELSE  0.1000 sec
.01
THE ABSORPTION COEFFICIENT, (ELSE 0.5E-03 per cm)

THE LAYER THICKNESS, (ELSE "IDEAL")

THE PARTICLE SIZE, (ELSE  1.00 um)

THE WAVELENGTH, (ELSE  0.4880 um)

THE %-AGE OF SOLID MATERIAL, (ELSE 75. %)

THE INDEX OF REFRACTION, (ELSE 1.460)

THE MAXIMUM ALLOWABLE TRANSMISSION %age, IF ANY.
```

Appendix B: Sample Model Output

FOR Xi= 0.932mm, 0.04086 % IS TRANSMITTED, AND 0.04086 % IS ABSORBED

TEMPERATURE PROFILE

	RADII (cm.)							
TIME (s.)	0.00	0.14	0.17	0.20	0.25	0.33	0.50	1.00
0.010	483.1	300.1	300.1	300.1	300.1	299.9	300.1	300.0
0.020	601.1	300.1	300.1	300.1	300.1	299.9	300.1	300.0
0.030	686.6	300.1	300.2	300.2	300.1	299.8	300.2	300.0
0.040	753.5	300.1	300.2	300.2	300.1	299.8	300.3	300.0
0.050	808.4	300.1	300.2	300.2	300.1	299.8	300.3	300.0
0.060	854.9	300.1	300.2	300.2	300.1	299.8	300.3	300.0
0.070	895.3	300.1	300.2	300.2	300.1	299.8	300.4	300.0
0.080	930.9	300.1	300.2	300.2	300.1	299.8	300.4	300.0
0.090	962.8	300.1	300.2	300.2	300.1	299.8	300.4	300.0
0.100	991.7	300.1	300.2	300.2	300.1	299.8	300.4	300.0
0.120	1042.3	300.1	300.2	300.2	300.1	299.8	300.4	300.0
0.160	1123.7	300.1	300.2	300.2	300.1	299.8	300.5	300.0
0.200	1187.8	300.1	300.2	300.2	300.1	299.8	300.5	300.0
0.240	1240.7	300.1	300.2	300.2	300.1	299.8	300.5	300.0
0.280	1285.7	300.1	300.2	300.2	300.1	299.8	300.5	300.0
0.320	1325.0	300.1	300.2	300.2	300.1	299.8	300.5	300.0
0.360	1359.7	300.1	300.2	300.2	300.1	299.8	300.5	300.0
0.400	1390.9	300.1	300.2	300.2	300.1	299.8	300.5	300.0
0.440	1419.1	300.1	300.2	300.2	300.1	299.8	300.5	300.0
0.480	1445.0	300.1	300.2	300.2	300.1	299.8	300.5	300.0
0.520	1468.8	300.1	300.2	300.2	300.1	299.8	300.5	300.0
0.560	1490.9	300.1	300.2	300.2	300.1	299.8	300.5	300.0
0.600	1511.5	300.1	300.2	300.2	300.1	299.8	300.5	300.0
0.640	1530.8	300.2	300.2	300.2	300.1	299.8	300.5	300.0
0.680	1548.9	300.2	300.2	300.2	300.1	299.8	300.5	300.0
0.720	1566.0	300.2	300.2	300.2	300.1	299.8	300.5	300.0
0.760	1582.2	300.3	300.2	300.2	300.1	299.8	300.5	300.0
0.800	1597.6	300.4	300.2	300.2	300.1	299.8	300.5	300.0
0.840	1612.2	300.5	300.2	300.2	300.1	299.8	300.5	300.0
0.880	1626.2	300.6	300.2	300.2	300.1	299.8	300.5	300.0
0.920	1639.5	300.7	300.3	300.2	300.1	299.8	300.5	300.0
0.960	1652.3	300.9	300.3	300.2	300.1	299.8	300.5	300.0
1.000	1664.6	301.1	300.3	300.2	300.1	299.8	300.5	300.0
1.040	1676.4	301.3	300.4	300.2	300.1	299.8	300.5	300.0
1.080	1687.7	301.5	300.5	300.2	300.1	299.8	300.5	300.0
1.120	1698.7	301.8	300.5	300.2	300.1	299.8	300.5	300.0
1.160	1709.3	302.1	300.6	300.2	300.1	299.8	300.5	300.0
1.200	1719.5	302.4	300.7	300.2	300.1	299.8	300.5	300.0
1.240	1729.3	302.7	300.8	300.2	300.1	299.8	300.5	300.0
1.280	1738.9	303.1	300.9	300.2	300.1	299.8	300.5	300.0
1.320	1748.2	303.5	301.0	300.3	300.1	299.8	300.5	300.0
1.360	1757.2	303.9	301.2	300.3	300.1	299.8	300.5	300.0

1.400	1765.9	304.4	301.3	300.3	300.1	299.8	300.5	300.0
1.440	1774.4	304.8	301.5	300.3	300.1	299.8	300.5	300.0
1.480	1782.7	305.3	301.7	300.4	300.1	299.8	300.5	300.0
1.520	1790.7	305.9	301.9	300.4	300.1	299.8	300.5	300.0
1.560	1798.6	306.4	302.1	300.4	300.1	299.8	300.5	300.0
1.600	1806.2	307.0	302.3	300.5	300.1	299.8	300.5	300.0
1.640	1813.7	307.6	302.5	300.5	300.1	299.8	300.5	300.0
1.680	1820.9	308.2	302.8	300.6	300.1	299.8	300.5	300.0
1.720	1828.0	308.8	303.0	300.7	300.1	299.8	300.5	300.0
1.760	1835.0	309.5	303.3	300.7	300.2	299.8	300.5	300.0
1.800	1841.8	310.1	303.6	300.8	300.2	299.8	300.5	300.0
1.840	1848.4	310.8	303.9	300.9	300.2	299.8	300.5	300.0
1.880	1854.9	311.5	304.2	301.0	300.2	299.8	300.5	300.0
1.920	1861.3	312.3	304.6	301.1	300.2	299.8	300.5	300.0
1.960	1867.5	313.0	304.9	301.2	300.2	299.8	300.5	300.0
2.000	1873.6	313.8	305.3	301.3	300.2	299.8	300.5	300.0

THE CENTRAL TEMPERATURE IS: 1873.59 K

THE MAXIMUM POWER DENSITY IS : 28.8222 MW/cm2

IT TOOK 3 STEPS TO FIND THE POWER

Appendix C: FORTRAN Source Code

```
THIS PROGRAM GENERATES A MODEL OF THE SCATTERING PROPERTIES OF A LAYER

      PROGRAM LAYER
      IMPLICIT REAL*8 (A-H,J,L,N,O-Z)
      REAL*8    XR(10),RR(10),B(10000),K,T(10,1000),TIME(1000)
      LOGICAL  NOTMAX, NOX, HIGH, POWER
      EXTERNAL J0
      COMMON/ BETA / B

      ZRO= 0.D0
      HAF= .5D0
      ONE= 1.D0
      TWO= 2.D0
      PI=  3.1415926535897 93D0

THESE PARAMETERS CAN BE VARIED, DEPENDING ON THE MATERIAL

      OPEN(10,STATUS='NEW',FILE='LAYER.DAT')
      K=    .26D0
      SIGMA=     5.67D-8
      SIGMA=     ZRO
      H34= 8.1D9
      H34= ZRO
      RHO= 2.65D3
      CTH= 794.
      ALPHA=     K / (RHO*CTH)

      H3=  3.D2
      IRM= 8
      IRM0=      IRM
      IR2= NINT( 4.5 * IRM )
      CALL BETA0

      CA0= 5.D-4
      S0=  ONE
      L0=  .488D0
      PP0= 75.D0
      N0=  1.46D0
      TMELT0=    2200.
      R0=  ONE
      RB0= .1D0
      TYM0=      1.D1
      DT0= 1.D-1
      X0=  ONE
      P1=  1.D2

      WRITE(6,20) TMELT0
      READ(5,120) TMELT
      IF( TMELT .LE. ZRO ) TMELT=  TMELT0
      TMELT0=    TMELT

C
      WRITE(6,32) RB0
```

```
      READ(5,120) RB
      IF( RB .LE. ZRO ) RB=  RB0
      RB0= RB
      RB=  RB * .5D-2
C
      WRITE(6,21) R0
      READ(5,120) R
      IF( R .LE. ZRO ) R=  R0
      R0=  R
      R=   R * .5D-2
C
      WRITE(6,22) TYM0
      READ(5,120) TYM
      IF( TYM .LE. ZRO ) TYM=  TYM0
      TYM0=     TYM
C
      WRITE(6,29) DT0
      READ(5,120) DT
      IF( DT .LE. ZRO ) DT=  DT0
      DT0= DT
C
      WRITE(6,91)  CA0
      READ(5,120)  CA
      IF( CA .LE. 0.D0 ) CA= CA0
      CA0= CA
C
      WRITE(6,92)
      READ(5,120)  X
      NOX= X .LE. 0.D0
      X=   X * .1
C
      WRITE(6,93)  S0
      READ(5,120)  S
      IF( S .LE. 0.D0 ) S= S0
      S0=  S
      S=   S * 1.D-4
C
      WRITE(6,94)  L0
      READ(5,120)  L
      IF( L .LE. 0.D0 ) L= L0
      L0=  L
      L=   L * 1.D-4
C
      WRITE(6,95)  PP0
      READ(5,120)  PP
      IF( PP .LE. 0.D0 ) PP= PP0
      PP0= PP
      PP=  PP * 1.D-2
C
      WRITE(6,96)  N0
      READ(5,120)  N
      IF( N .LE. 0.D0 ) N= N0
      N0=  N
C
```

```
      WRITE(6,97)
      READ(5,120)  TMAX
      NOTMAX= TMAX .LE. 0.D0
      TMAX=      TMAX / 1.D2
C
      Y=    9.D0 * PP * ( 11.D0*PP - 8.D0*PP*PP - 3.D0)
      Y=    (N-ONE) * Y / (L/S + DLOG10(S/L))
      CT=   Y / ( N * S )
      CA=   1.D1 * CA
      CR=   CT - CA
C
      C=    DSQRT( CA * (CT+CR) )
      Q=    (CA + CR + C) / CR
      QP1=  Q + 1
      QM1=  Q - 1
      Q2M=  QP1 * QM1
C
      XI=   QP1 + DSQRT( QP1*QP1 - 1 )
      XI=   DLOG( XI ) - DLOG( Q )
      XI=   XI / C
C
      EX=   DEXP( C * XI )
      TI=   1.D2 * Q2M * EX / ( Q * Q * EX * EX - 1 )
      AI=   1.D2 * QM1 * ( EX - 1 ) / ( Q * EX + 1 )
      XI=   1.D1 * XI
      X0=   XI
      ABS=  AI * 1.D-2
      WRITE(6,98) XI, TI, AI
      WRITE(10,98) XI, TI, AI
:
      IF( NOX ) GO TO  5
      EX=   DEXP( C * X )
      AX=   1.D2 * QM1 * ( EX - 1 ) / ( Q * EX + 1 )
      TX=   1.D2 * Q2M * EX / ( Q * Q * EX * EX - 1 )
      X=    X * 1.D1
      X0=   X
      ABS=  AX * 1.D-2
      WRITE(6,99) X, TX, AX
      WRITE(10,99) X, TX, AX
:
    5 IF( NOTMAX ) GO TO  10
      XT=   Q2M*Q2M + 4*Q*Q*TMAX*TMAX
      XT=   Q2M + DSQRT( XT )
      XT=   XT / ( 2 * Q * Q * TMAX )
      XT=   DLOG( XT ) / C
      EX=   DEXP( C * XT )
      AT=   1.D2 * QM1 * ( EX - 1 ) / ( Q * EX + 1 )
      TT2=  1.D2 * Q2M * EX / ( Q * Q * EX * EX - 1 )
      XT=   XT * 1.D1
      X0=   XT
      ABS=  AT * 1.D-2
      WRITE(6,99) XT, TT2, AT
      WRITE(10,99) XT, TT2, AT
:
```

```
C  THIS SECTION CALCULATES THE MAXIMUM BEAM POWER BEFORE MELTING
C
  10 X=    X0 * 1.D-3
     RHO= RHO * PP
     BF=  RB / R
     P2=  P1 / (PI * RB * RB)
C
     DO 45 I=2,IRM
     XR(I)=     ONE / (ONE+IRM-I)
  45 RR(I)=     XR(I) * R * 1.D2
     XR(1)=     XR(IRM) * BF
     RR(1)=     XR(1) * R * 1.D2
C
     ITM= NINT( TYM / DT )
     RAD1=      SIGMA * DT / ( RHO * CTH * X )
     EXP1=      ALPHA * DT / ( R * R )
     TEM0=      ALPHA * DT * BF * BF * ABS / (K * X)
C
C LOOP OVER POWER, TO FIT FINAL TEMPERATURE
C
     T1=  ZRO
     TG=  1.D7
     PG=  1.D13
     POWER=     .FALSE.
     HIGH=      .FALSE.
     IRM= 1
C
     DO 350 IP=1,999
     TEM1=      TEM0 * P2
C
     DO 50  IT=1,ITM
     DO 50  IR=1,IRM
  50 T(IT,IR)= H3
C
C LOOP OVER RADIUS
C
     IF( POWER ) IRM=  IRM0
     DO 300 IR=1,IRM
C
C LOOP OVER TIME
C
     TOLD=      H3
     DO 300 IT=1,ITM
     TIME(IT)= IT * DT
     BEXP=      EXP1 * IT
     RAD= ZRO
C
C THIS SECTION CALCULATES THE SUMMATION TERM
C
 100 SUM= ZRO
     DO 200 I=1,9999
     DSUM=      J0(I,XR(IR)) * DEXP( -BEXP*B(I)*B(I) )
     SUM = SUM + DSUM
     IF( DABS(DSUM) .LT. DABS(1.D-6*SUM) )  GO TO 250
```

```
 200 CONTINUE
     WRITE(6,28) IP
C
C THIS SECTION CALCULATES THE RADIATIVE LOSSES
C
 250 TEMP=      TEM1 * ( ONE + SUM )
     TT=  TOLD + TEMP * HAF
     IF( TT .GT. 1.D8 ) WRITE(6,*) IR, IT, TOLD, TEMP
     T4=        TT**4
     RAD= RAD1 * (T4 - H34)
     IF( RAD .GT. TT ) RAD=  TT
     TOLD=      TEMP - RAD + TOLD
     T(IR,IT)= TOLD
 300 CONTINUE
C
     P3=  P2 * 1.D-10
     WRITE(6,*) IP, P3, RAD
     WRITE(6,*) (T(IR,1),IR=1,IRM)
     WRITE(6,*) (T(IR,ITM),IR=1,IRM)
C
     T2=  T(1,ITM)
     IF( POWER ) GO TO  375
     IF( IP .GT. 1 ) GO TO  325
     TL=  T(1,ITM)
     PL=  P2
     P2=  5.D0 * (TMELT - H3) * P2 / (TL - H3)
     GO TO  350
C
C TEST FOR TEMPERATURE WITHIN CRITICAL VALUE
C
 325 POWER=     T2.LE.TMELT .AND. T2.GT.TMELT*.99
     IF( POWER ) GO TO  350
     IF( HIGH .OR. T2.GT.TMELT ) GO TO  330
     P2=  1.D1 * P2
     GO TO  350
C
 330 HIGH=      .TRUE.
     IF( T2 .GT. TMELT ) TG= T2
     IF( T2 .GT. TMELT ) PG= P2
     IF( T2 .LT. TMELT ) TL= T2
     IF( T2 .LT. TMELT ) PL= P2
     DTEM=      TG - TL
     DTMELT=    TMELT*.995 - TL
     DP=  PG - PL
     P2=  PL + DP * DTMELT / DTEM
 350 CONTINUE
C
C WRITE TEMPERATURE DISTRIBUTION AND MAXIMUM POWER
C
 375 CONTINUE
     WRITE(10,26) (RR(I),I=1,IRM)
     DO 400 IT=1,10
     IF( IT .GT. ITM ) GO TO  500
 400 WRITE(10,121) TIME(IT), (T(IR,IT), IR=1,IRM)
```

```
      IDT= MAX( ITM/50 , 1 )
      DO 450 IT=11,ITM
      IF( IT .GT. ITM ) GO TO  500
      IF( MOD(IT,IDT) .NE. 0 ) GO TO  450
      WRITE(10,121) TIME(IT), (T(IR,IT), IR=1,IRM)
  450 CONTINUE
C
  500 WRITE(6,25) T2, P3
      WRITE(10,25) T2, P3
      WRITE(10,27) IP
      STOP
   20 FORMAT(' ENTER THE MAXIMUM ALLOWABLE TEMPERATURE, ELSE ',F7.2,'K')
   21 FORMAT(' THE DIAMETER OF THE LAYER, ELSE ',F7.2,' cm')
   22 FORMAT(' THE TIME THE BEAM IS ON TARGET, ELSE ',F7.2,' sec')
   23 FORMAT(' THE TOTAL ABSORPTION, ELSE ',E7.1)
   24 FORMAT(' THE LAYER THICKNESS, ELSE ',F7.2,' mm')
   25 FORMAT(/,' THE CENTRAL TEMPERATURE IS: ',F7.2,'K',
     & //,' THE MAXIMUM POWER DENSITY IS :'F9.4,' MW/cm2')
   26 FORMAT(/,20X,'TEMPERATURE PROFILE',//,8X,<IR2>X,'RADII (cm.)',
     & /,' TIME (s.)',8(F7.2,2X),/,' ----------',<IRM>(2X,'-----',2X))
   27 FORMAT(/,' IT TOOK ',I4,' STEPS TO FIND THE POWER')
   28 FORMAT(' THE SUM LOOP EXCEEDED 9999 TERMS')
   29 FORMAT(' THE TIME INCREMENT, ELSE ',F7.4,' sec')
   31 FORMAT(' RADIATION: ',F9.2,' EXCEEDED TEMPERATURE: ',F9.2)
   32 FORMAT(' THE DIAMETER OF THE BEAM, ELSE ',F7.3,' cm')
   33 FORMAT(' THE POWER DENSITY ',F9.2,' KW, GAVE A TEMPERATURE
     & ',F7.2,'K,',/,' WHICH WAS LESS THAN THE MAX. TEMPERATURE
     & ',F7.2,'K')
   91 FORMAT(' THE ABSORPTION COEFFICIENT, (ELSE ',E7.1,' per cm)')
   92 FORMAT(' THE LAYER THICKNESS, IN mm (ELSE "IDEAL")')
   93 FORMAT(' THE PARTICLE SIZE, (ELSE ',F5.2,' um)')
   94 FORMAT(' THE WAVELENGTH, (ELSE ',F7.4,' um)')
   95 FORMAT(' THE %-AGE OF SOLID MATERIAL, (ELSE ',F3.0,' %)')
   96 FORMAT(' THE INDEX OF REFRACTION, (ELSE ',F5.3,')')
   97 FORMAT(' THE MAXIMUM ALLOWABLE TRANSMISSION %age, IF ANY.')
   98 FORMAT(' FOR Xi= ',F7.3,'mm,  ',F8.5,' % IS TRANSMITTED,  AND ',
     & F8.5,' % IS ABSORBED')
   99 FORMAT(' FOR X=  ',F7.3,'mm,  ',F8.5,' % IS TRANSMITTED,  AND ',
     & F8.5,' % IS ABSORBED')
  120 FORMAT(3F25.16)
  121 FORMAT(1X,F7.3,8(1X,F8.1))
      END
C
```

```
C
C
  THIS SUBROUTINE CALCULATES   Jo(xB)/Jo(B)**2
C
      FUNCTION J0(I, XX)
      IMPLICIT REAL*8 (A-H,J,O-Z)
      REAL*8  B(10000), J(9999), S(2)
      LOGICAL OLD
      COMMON/ BETA / B
      COMMON/ LOGIC / OLD
C
      ZRO= 0.D0
      ONE= 1.D0
      TWO= 2.D0
      PI=  3.1415926535897 93D0
      PO4= PI / 4.D0
C
      X=   XX * B(I)
      DO 30 IX=1,2
C
C APPROXIMATION FOR LARGE ARGUMENTS
C
      IF( X .LT. 6.D1 ) GO TO  5
      S(IX)=    DSQRT( TWO / (PI*X) )
      IF( IX .EQ. 1 ) S(IX)= S(IX) * DCOS( X - PO4 )
      GO TO  30

  REVERSE ITERATION FOR SMALL ARGUMENTS
C
    5 SUM= ZRO
      IMAX=     INT(9+1.83*X)
      J(IMAX+2)= ZRO
      J(IMAX+1)= 1.D-30
C
      DO 10 IM=IMAX,1,-1
      J(IM)=    TWO*IM*J(IM+1)/X - J(IM+2)
      IF(IM .EQ. 1) GO TO  20
   10 SUM= SUM + (1 + (-1)**(IM-1)) * J(IM)
C
   20 SUM= SUM + J(1)
      S(IX)=    J(1) / SUM
      X=   B(I)
   30 CONTINUE
C
      J0=  S(1) / (S(2)*S(2))
C     IF( .NOT. OLD ) WRITE(6,100)
      OLD= .TRUE.
C     WRITE(6,101) I, B(I), S(1), S(2), J0
      RETURN
  100 FORMAT('   I',8X,'B(I)',11X,'Jo(xB)',10X,'Jo(B)',12X,'J0')
  101 FORMAT(1X,I4,1X,4F16.10)

      END
C
```

```
      IDT= MAX( ITM/50 , 1 )
      DO 450 IT=11,ITM
      IF( IT .GT. ITM ) GO TO  500
      IF( MOD(IT,IDT) .NE. 0 ) GO TO  450
      WRITE(10,121) TIME(IT), (T(IR,IT), IR=1,IRM)
  450 CONTINUE
C
  500 WRITE(6,25) T2, P3
      WRITE(10,25) T2, P3
      WRITE(10,27) IP
      STOP
   20 FORMAT(' ENTER THE MAXIMUM ALLOWABLE TEMPERATURE, ELSE ',F7.2,'K')
   21 FORMAT(' THE DIAMETER OF THE LAYER, ELSE ',F7.2,' cm')
   22 FORMAT(' THE TIME THE BEAM IS ON TARGET, ELSE ',F7.2,' sec')
   23 FORMAT(' THE TOTAL ABSORPTION, ELSE ',E7.1)
   24 FORMAT(' THE LAYER THICKNESS, ELSE ',F7.2,' mm')
   25 FORMAT(/,' THE CENTRAL TEMPERATURE IS: ',F7.2,'K',
     & //,' THE MAXIMUM POWER DENSITY IS :'F9.4,' MW/cm2')
   26 FORMAT(/,20X,'TEMPERATURE PROFILE',//,8X,<IR2>X,'RADII (cm.)',
     & /,' TIME (s.)',8(F7.2,2X),/,' ---------',<IRM>(2X,'-----',2X))
   27 FORMAT(/,' IT TOOK ',I4,' STEPS TO FIND THE POWER')
   28 FORMAT(' THE SUM LOOP EXCEEDED 9999 TERMS')
   29 FORMAT(' THE TIME INCREMENT, ELSE ',F7.4,' sec')
   31 FORMAT(' RADIATION: ',F9.2,' EXCEEDED TEMPERATURE: ',F9.2)
   32 FORMAT(' THE DIAMETER OF THE BEAM, ELSE ',F7.3,' cm')
   33 FORMAT(' THE POWER DENSITY ',F9.2,' KW, GAVE A TEMPERATURE
     & ',F7.2,'K,',/,' WHICH WAS LESS THAN THE MAX. TEMPERATURE
     & ',F7.2,'K')
   91 FORMAT(' THE ABSORPTION COEFFICIENT, (ELSE ',E7.1,' per cm)')
   92 FORMAT(' THE LAYER THICKNESS, IN mm (ELSE "IDEAL")')
   93 FORMAT(' THE PARTICLE SIZE, (ELSE ',F5.2,' um)')
   94 FORMAT(' THE WAVELENGTH, (ELSE ',F7.4,' um)')
   95 FORMAT(' THE %-AGE OF SOLID MATERIAL, (ELSE ',F3.0,' %)')
   96 FORMAT(' THE INDEX OF REFRACTION, (ELSE ',F5.3,')')
   97 FORMAT(' THE MAXIMUM ALLOWABLE TRANSMISSION %age, IF ANY.')
   98 FORMAT(' FOR Xi= ',F7.3,'mm,  ',F8.5,' % IS TRANSMITTED,  AND ',
     & F8.5,' % IS ABSORBED')
   99 FORMAT(' FOR X=  ',F7.3,'mm,  ',F8.5,' % IS TRANSMITTED,  AND ',
     & F8.5,' % IS ABSORBED')
  120 FORMAT(3F25.16)
  121 FORMAT(1X,F7.3,8(1X,F8.1))
      END
C
```

```
C
C
C THIS SUBROUTINE CALCULATES   Jo(xB)/Jo(B)**2
C
      FUNCTION J0(I, XX)
      IMPLICIT REAL*8 (A-H,J,O-Z)
      REAL*8  B(10000), J(9999), S(2)
      LOGICAL OLD
      COMMON/ BETA / B
      COMMON/ LOGIC / OLD
C
      ZRO= 0.D0
      ONE= 1.D0
      TWO= 2.D0
      PI=  3.1415926535897 93D0
      PO4= PI / 4.D0
C
      X=   XX * B(I)
      DO 30 IX=1,2
C
C APPROXIMATION FOR LARGE ARGUMENTS
C
      IF( X .LT. 6.D1 ) GO TO  5
      S(IX)=    DSQRT( TWO / (PI*X) )
      IF( IX .EQ. 1 ) S(IX)= S(IX) * DCOS( X - PO4 )
      GO TO  30
C
C REVERSE ITERATION FOR SMALL ARGUMENTS
C
    5 SUM= ZRO
      IMAX=     INT(9+1.83*X)
      J(IMAX+2)= ZRO
      J(IMAX+1)= 1.D-30
C
      DO 10 IM=IMAX,1,-1
      J(IM)=    TWO*IM*J(IM+1)/X - J(IM+2)
      IF(IM .EQ. 1) GO TO  20
   10 SUM= SUM + (1 + (-1)**(IM-1)) * J(IM)
C
   20 SUM= SUM + J(1)
      S(IX)=    J(1) / SUM
      X=   B(I)
   30 CONTINUE
C
      J0=  S(1) / (S(2)*S(2))
C     IF( .NOT. OLD ) WRITE(6,100)
      OLD= .TRUE.
C     WRITE(6,101) I, B(I), S(1), S(2), J0
      RETURN
  100 FORMAT('   I',8X,'B(I)',11X,'Jo(xB)',10X,'Jo(B)',12X,'J0')
  101 FORMAT(1X,I4,1X,4F16.10)

      END
C
```

```
C
C  THIS SUBROUTINE ENTERS THE FIRST 18 ZEROS OF THE FIRST ORDER BESSEL
FUNCTION
C  FROM Abramowitz and Stegun "HANDBOOK OF MATHEMATICAL FUNCTIONS" AND
APPROXIMATES THE REST
C
      SUBROUTINE BETA0
      REAL*8 B(10000), PI
C
      COMMON/ BETA / B
C
      PI=  3.14159265358979 3D0
C
      B(1)=       3.8317059702
      B(2)=       7.0155866698
      B(3)=      10.1734681351
      B(4)=      13.3236919363
      B(5)=      16.4706300509
      B(6)=      19.6158585105
      B(7)=      22.7600843806
      B(8)=      25.9036720876
      B(9)=      29.0468285349
      B(10)=     32.1896799110
      B(11)=     35.3323075501
      B(12)=     38.4747662348
      B(13)=     41.6170942128
      B(14)=     44.7593189977
      B(15)=     47.9014608872
      B(16)=     51.0435351836
      B(17)=     54.1855536411
      B(18)=     57.3275254379
C
      DO 1 I=19,9999
    1 B(I)=      PI * (I + .25D0)
C
      RETURN
      END
```

DISTRIBUTION LIST

1 copy to:
COMMANDER
U.S. ARMY TRAINING AND DOCTRINE
COMMAND
ATTN: ATCD-SE
FT. MONROE, VA 23651

1 copy to:
PROGRAM MANAGER - CLOTHING AND
INDIVIDUAL EQUIPMENT
ATTN: AMCPM-CIE
WOODBRIDGE, VA 22194-4206

1 copy to:
COMMANDANT
U.S. ARMY INFANTRY SCHOOL
ATTN: ATSH-CD-ML-C
FT. BENNING, GA 31905

1 copy to:
COMMANDANT
U.S. ARMY ARMOR SCHOOL
ATTN: ATSB-CD-ML
FT. KNOX, KY 40121-5215

1 copy to:
COMMANDANT
U.S. ARMY CHEMICAL SCHOOL
ATTN: ATZN-CM-CS
FT. McCLELLAN, AL 36205-5000

1 copy to:
COMMANDANT
U.S. ARMY AVIATION SCHOOL
ATTN: ATZQ-CDM-C
FT. RUCKER, AL 36362

1 copy to:
COMMANDER
U.S. ARMY NUCLEAR AND
CHEMICAL AGENCY
ATTN: MONA-NU BLDG. 2073
7500 BACKLICK ROAD
SPRINGFIELD, VA 22150-3198

1 copy to:
COMMANDER
U.S. ARMY NUCLEAR AND
CHEMICAL AGENCY
ATTN: MONA-ZB BLDG. 2073
7500 BACKLICK ROAD
SPRINGFIELD, VA 22150-3198

1 copy to:
DIRECTOR
DEFENSE NUCLEAR AGENCY
ATTN: TDTR
6801 TELEGRAPH ROAD
ALEXANDRIA, VA 23310

1 copy to:
DIRECTOR
DEFENSE NUCLEAR AGENCY
ATTN: HRP
6801 TELEGRAPH ROAD
ALEXANDRIA, VA 23310-3398

1 copy to:
HQDA
OFFICE OF THE SURGEON GENERAL
ATTN: DASG-HCD
5109 LEESBURG PIKE
FALLS CHURCH, VA 22041-3258

1 copy to:
COMMANDER
U.S. ARMY COMBINED ARMS DEFENSE CENTER
ATTN: ATZL-CAD-N
FT. LEAVENWORTH, KS 66027-5300

1 copy to:
U.S. ARMY AVIATION MEDICAL RESEARCH
LABORATORY
ATTN: SGRD-VAB-CB
FT. RUCKER, AL 36352-5000

1 copy to:
COMMANDER
WALTER REED INSTITUTE OF RESEARCH
ATTN: SGRD-UWZ
WASHINGTON, DC 20307-5100

1 copy to:

U.S. ARMY LABORATORY COMMAND
HARRY DIAMOND LABORATORIES
ATTN: SLCHD-NW-TN
2800 POWDER MILL ROAD
ADELPHI, MD 20783

1 copy to:

U.S. NAVY CLOTHING AND TEXTILE
RESEARCH FACILITY
ATTN: CODE 40.1
21 STRATHMORE ROAD
NATICK, MA 01760-2490

2 copies to:

DEFENSE TECHNICAL INFORMATION CENTER
CAMERON STATION
ALEXANDRIA, VA 22314

4 copies to:

COMMANDER
U.S. ARMY NATICK RD&E CENTER
TECHNICAL LIBRARY
ATTN: STRNC-MIL
NATICK, MA 01760

1 copy to:

COMMANDER
U.S. ARMY NATICK RD&E CENTER
ATTN: STRNC-MSR
NATICK, MA 01760-5020

45 copies to:

COMMANDER
U.S. ARMY NATICK RD&E CENTER
ATTN: STRNC-YSD (Mr. G. Caldarella)
NATICK, MA 01760-5020